

NASA CR-134398

FINAL REPORT
CONTRACT NAS9-13568
JUNE 28, 1974

ASYMMETRICAL BOOSTER ASCENT
GUIDANCE AND CONTROL
SYSTEM DESIGN STUDY

VOLUME I
SUMMARY

N74-32299
UNCLASSIFIED
46961
G3/31
CSCL 22B
(NASA-CR-134398) ASYMMETRICAL BOOSTER
ASCENT GUIDANCE AND CONTROL SYSTEM DESIGN
STUDY. VOLUME 1: SUMMARY Final
Report (Boeing Aerospace Co., Houston,
Tex.) 83 p HC \$7.25



5-2581-HOU-154

CONTRACT NAS9-13568

ASYMMETRICAL BOOSTER ASCENT
GUIDANCE AND CONTROL
SYSTEM DESIGN STUDY

VOLUME I

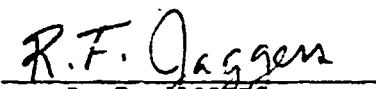
SUMMARY

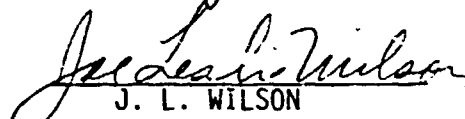
JUNE 28, 1974

PREPARED BY


F. E. WILLIAMS


R. S. LEMON


R. F. JAGGERS


J. L. WILSON

APPROVED BY


W. G. RYALS
PROGRAM MANAGER

PREFACE

Final report of Asymmetrical Booster Ascent Guidance and Control System Design Studies performed under Contract NAS9-13568 are contained in five separate volumes identified as follows:

- Volume I - Summary
- Volume II - SSFS Math Models - Ascent
- Volume III - Space Shuttle Vehicle SRB Actuator Failure Study
- Volume IV - Sampled Data Stability Analysis Program (SADSAP) -
Users Guide
- Volume V - Space Shuttle Powered Explicit Guidance

ABSTRACT

Volume I is a summary of the Asymmetrical Booster Ascent Guidance and Control System Design Studies. Contained in this volume are brief descriptions of volumes II, III, IV and V, and the Space Shuttle Stability Analysis.

KEY WORDS

Flight Dynamics

Space Shuttle

Stability Analysis

Nichols Plots

Guidance

TABLE OF CONTENTS

PREFACE	ii
ABSTRACT AND ACKNOWLEDGEMENTS	iii
KEY WORDS	iii
TABLE OF CONTENTS	iv
LIST OF ILLUSTRATIONS	v
1.0 INTRODUCTION AND SUMMARY	1
2.0 DYNAMICS AND CONTROL ANALYSIS	2
2.1 Simulation Development	2
2.2 Analysis	7
2.3 Simulation Calibration	9
3.0 STABILITY ANALYSIS	10
3.1 Summary	10
3.2 Sampled Data Stability Analysis Program	11
3.3 Space Shuttle Pitch Axis Equations of Motion	12
3.4 Space Shuttle Lateral Axes Equations of Motion	21
3.5 Rigid Body Stability Analysis	37
3.6 Bending Stability	62
3.7 Dog Wags Tail	69
4.0 GUIDANCE ANALYSIS	75

LIST OF ILLUSTRATIONS

Figure 1	DESIGN CONDITIONS	8
Figure 2	PITCH AXES NICHOLS PLOT AT IGNITION	38
Figure 3	PITCH AXES NICHOLS PLOT AT 60 SECONDS	39
Figure 4	PITCH AXES NICHOLS PLOT AT MAX Q	40
Figure 5	PITCH AXES NICHOLS PLOT AT 70 SECONDS	41
Figure 6	PITCH AXES NICHOLS PLOT AT 95 SECONDS	42
Figure 7	PITCH AXES NICHOLS PLOT AT 115 SECONDS	43
Figure 8	PITCH AXES NICHOLS PLOT AT 120 SECONDS	44
FIGURE 9	PITCH AXES NICHOLS PLOT AT SRM BURNOUT	45
Figure 10	YAW AXES NICHOLS PLOT AT IGNITION	46
Figure 11	YAW AXES NICHOLS PLOT AT 60 SECONDS	47
Figure 12	YAW AXES NICHOLS PLOT AT MAX Q	48
Figure 13	YAW AXES NICHOLS PLOT AT 70 SECONDS	49
Figure 14	YAW AXES NICHOLS PLOT AT 95 SECONDS	50
Figure 15	YAW AXES NICHOLS PLOT AT 115 SECONDS	51
Figure 16	YAW AXES NICHOLS PLOT AT 120 SECONDS	52
Figure 17	YAW AXES NICHOLS PLOT AT SRM BURNOUT	53
Figure 18	ROLL AXES NICHOLS PLOT AT IGNITION	54
Figure 19	ROLL AXES NICHOLS PLOT AT 60 SECONDS	55
Figure 20	ROLL AXES NICHOLS PLOT AT MAX Q	56
Figure 21	ROLL AXES NICHOLS PLOT AT 70 SECONDS	57
Figure 22	ROLL AXES NICHOLS PLOT AT 95 SECONDS	58
Figure 23	ROLL AXES NICHOLS PLOT AT 115 SECONDS	59
Figure 24	ROLL AXES NICHOLS PLOT AT 120 SECONDS	60
Figure 25	ROLL AXES NICHOLS PLOT AT SRM BURNOUT	61

LIST OF ILLUSTRATIONS (Continued)

Figure 26	PITCH AXES NICHOLS PLOT AT MAX Q-6 BENDING MODES	65
Figure 27	PITCH AXES NICHOLS PLOT AT MAX Q-6 BENDING MODES - FILTERS	66
Figure 28	PITCH AXES NICHOLS PLOT AT MAX Q-6 BENDING MODES - SLOSH TO BENDING AND BENDING TO SLOSH	67
Figure 29	PITCH AXES NICHOLS PLOT AT MAX Q-6 BENDING MODES - SLOSH TO BENDING AND BENDING TO SLOSH - FILTERS	68
Figure 30	SSME TVC ACTUATOR BLOCK DIAGRAM	70
Figure 31	FREQUENCY RESPONSE OF DOG WAGS TAIL ACTUATOR TRANSFER FUNCTION	71
Figure 32	PITCH AXES NICHOLS PLOT AT MAX Q-6 BENDING MODES - SLOSH TO BENDING AND BENDING TO SLOSH - DWT	73
Figure 33	PITCH AXES NICHOLS PLOT AT MAX Q-6 BENDING MODES - SLOSH TO BENDING AND BENDING TO SLOSH - DWT - FILTERS	74

LIST OF TABLES

Table I	PITCH BENDING DATA AT MAX Q	63
Table II	FILTER TRANSFER FUNCTIONS	64

1.0 INTRODUCTION

This report documents in five volumes the principal accomplishments of the Asymmetrical Booster Ascent Guidance and Control System Design Studies and is the final report for contract NAS9-13568.

Volume I is a summary report of all five volumes and is intended to provide a quick reference to the entire report. Volume II contains the mathematical models developed by the Boeing Aerospace Company for use in rigid body and flexible body versions of the NASA JSC Space Shuttle Functional Simulator. Volume III documents the analyses performed to provide data for use in engine actuator and control system design. Section 2 of this Volume I summarizes simulation development and actuator failure analysis.

Space Shuttle stability analysis is presented in Section 3 with equations of motion for both pitch and lateral axes. The computer program used to obtain stability margins is described in detail in Volume IV, "The Sampled Data Stability Analysis Program Users Guide."

Section 4 discusses the guidance equation development for the Space Shuttle Powered Flight Phases. This work is documented in detail in Volume V.

2.0 Dynamics and Control Analysis

Under this contract extensive simulation development was accomplished for boost to orbit dynamics and control analysis. Vehicle configuration data were periodically updated, new and revised math models were developed, and the Space Shuttle Functional Simulator (SSFS) was modified and checked out. In addition, a new computer program was developed to automatically convert aerodynamic data into a form usable by the SSFS. Analyses were performed providing data for use in engine actuator and control system design.

2.1 Simulation Development

The Space Shuttle Functional Simulator (SSFS) is the principle tool used for dynamics and control analysis. During this contract the SSFS was periodically updated to the latest vehicle configuration as data became available. Math models were revised and new models were developed. These different versions of the SSFS were modified and checked out to provide: (1) Six degree-of-freedom first stage with three degree-of-freedom upper stages, (2) six degree-of-freedom simulation from lift-off to orbit insertion, (3) flexible body first stage simulation. An aero data program was developed that will read aerodynamic data from a magnetic tape, manipulate the data, and provide punched cards suitable for direct input to the SSFS. These developments are discussed in more detail in the succeeding paragraphs.

2.1.1 Configuration Data

Vehicle configuration data, as received, is not in proper form for use in the SSFS. Coordinate systems, reference locations, and units, are not standardized among the technologies; so the Aero, Mass, Propulsion and Geometric data must be converted prior to implementation into the computer program.

The references itemized here contain the converted data currently implemented in the SSFS.

- 1) Boeing Memo 5-2581-HOU-119, dated 7/19/73, tabulates the first stage mated vehicle aerodynamic data, including power on base drag and groundwind aero.
- 2) Boeing Memo 5-2581-HOU-121, dated 7/23/73, contains a listing of the data cards prepared from the preceding memo.
- 3) Boeing Memo 5-2581-HOU-128, dated 10/2/73, contains the configuration IV second stage mass properties and aerodynamic characteristics.
- 4) Boeing Memo 5-2581-HOU-129, dated 10/2/73, contains mass data for the due East launch, and all propulsion and TVC data including engine locations and coordinate system description.

Punched cards were prepared from these data and transmitted to Lockheed Electronics Corporation where they were written onto the master SSFS program tapes.

2.1.2 Math Models

The Boeing developed math models for use in SSFS are documented in Volume II of this report. During this contract period the following models were added.

- 1) Accel - Calculates acceleration for accelerometers located anywhere on the vehicle.
- 2) Momentum transfer at staging (added to ACTVEH)
- 3) BLC (Baseline Control System) was revised to reflect the latest configuration. Added models are:
 - a) Roll Command Filter
 - b) Accelerometer Filters
 - c) Mixing Logic Coefficients for Seven Engines
 - d) SRB Actuator Command Model Permitting Rotation of the Gimbals so the Direction of actuator Travel can be Arbitrarily set to any Angle without Affecting the Control System
 - e) OMS Engines Command Output
- 4) FLTSEQ (Flight Sequencing) provides consistent logic, including time delays, for staging commands issued by the flight software to the vehicle systems.
- 5) GUIDE - Unified Linear Tangent Guidance
- 6) THRCMD - Throttle Command - Throttle the Orbiter engines to limit acceleration to 3g.
- 7) "DOG WAGS TAIL" and actuator limiting were added to the flexible body engine forces model (derivation of this model is contained in Boeing Memo 5-2581-HOU-124).

In addition to these new models; AERO, CGAINS, MASPRO, MAXMIN, THRUST, and TVC were revised to permit full 6 DOF boost to orbit simulation.

2.1.3 SSFS Modifications and Checkout

2.1.3.1 Rigid Body

There currently exist two rigid body versions of the SSFS boost program:

1) Six degree-of-freedom first stage with three degree-of-freedom upper stage (6D-3D), 2) six degree-of-freedom from liftoff to orbit insertion (6D-6D).

When the 6D-6D is completely checked out it will have a 3D option for the upper stages and the 6D-3D version will be retired. The modifications made to the 6D-3D program were also given to Lockheed Electronics Corporation (LEC) for use in the 6D-6D program.

The 6D-3D program was checked out and determined to be operational on the Exec 8 computer system. The control gains calculating subroutine (c Gains) and the control system (BLC) were modified to incorporate updated engine deflection logic. When the G&C data book and the Rockwell control system were received, Boeing was directed to modify the program to that configuration so studies could be performed. These modifications consisted of: Adding acceleration calculations; adding filters for roll command and acceleration signals; providing roll-yaw coupling in the control system; providing for a 45° - 135° SRM actuator orientation in the control system and in thrust; adding a first order lag in the thrust vector control system, and also calculating and outputting the actuator duty cycles; changing the staging logic so staging could not occur until thrust and body criteria were met; and modifying the program logic to print out data at the actual staging time as well as the nominal time.

The 6D-6D program was checked at various stages of development. As originally received, the staging was rudimentary, with no provision for switching to upper stage aerodynamics or control. The program listings were marked to indicate desired modifications and returned to LEC. At the next check specific annotations were made illustrating program modifications to incorporate OMS capability into the simulator. LEC then proceeded to program for the complete upper stage flight, including the coast period, external tank jettison and OMS burn, and to incorporate the guidance described in Volume V, as well as the 6D-3D mods discussed above. The latest checkout revealed the need for more flexible flight sequencing. The logic was developed and the program listings were marked in detail, involving significant changes to the control system, mass properties subroutine, TVC, and equations of motion. This flight sequencing: 1) permits the flight software to command all major events; and 2) provides for simulation of time delays between command and action.

2.1.3.2 Flexible Body Checkout

A flexible body check run, program listings and program deck were received from LEC. The listings were examined and marked for correction as described in Boeing Memo 5-2581-HOU-122. The affected subroutines were ACTVEH, THRUST, TVC, AERO and BEND. As each subroutine was completed it was reexamined for correctness. Then working together with the LEC programmer, dynamic checkout runs were performed. During this checkout special printout was provided which will remain as a permanent feature to be output at the user's option. The print provides a diagnostic tool for simulation stability testing as well as providing hand calculating capability.

The simulation runs were compared with hand calculations and the remaining errors were detected and corrected. Several computation cycle times were tested to assure that the high speed loops used for the engines and bending would automatically adjust themselves to complete their calculations at the correct time.

Rockwell bending data was implemented in the program after appropriate coordinate system transformations were performed. The vehicle proved to be unstable and additional simulation testing awaits design and implementation of control filters (and revised bending data).

Boeing Memo 5-2581-HOU-127 describes the rate limiting procedure used in the thrust vector control system of the flexible body simulation. It was designed to prevent integrator instability and is incorporated in the model in Volume II.

2.1.4 Aero Data Program

The Aero Coefficient Generator (ACG) program has been developed to allow conversion of Space Shuttle aerodynamic data, available on magnetic tape, to linearized point-slope form. The program produces punched cards of the data, formatted in data statements for direct input into the NASA-JSC Space Shuttle Functional Simulator (SSFS) computer program. The program is documented in Boeing memo 5-2581-HOU-156 dated June 28, 1974.

2.2 Analysis

Studies were conducted investigating the performance of the Configuration IV Space Shuttle vehicle with one solid rocket motor TVC actuator failure. Primary study objectives were to determine design cases (worst conditions) for the baseline TVC actuator configuration (45° - 135° orientation) and the 0° - 90° TVC (pitch-yaw) configuration. These studies are documented in Volume III.

Simulations were performed, individually failing each of the four solid rocket booster (SRB) actuators. Several failure times were tested, from liftoff to the region of maximum dynamic pressure (Q_{max}). Thrust unbalance between the two SRM's was simulated and the effect of headwinds, tailwinds and crosswinds was investigated. Staging criteria were implemented in the simulation. Nominal staging for this configuration occurs at 123 seconds from liftoff. All simulation runs that failed to meet the staging criteria were terminated at 140 seconds.

It was determined that the worst case design conditions for this vehicle configuration are those summarized in Figure 1. For those mid-boost conditions (liftoff to beyond Max Q) the loads indicator, dynamic pressure times sideslip angle ($Q\beta$) was significantly higher than for other simulation cases. Satisfactory compensation was achieved for the mid-boost cases.

At thrust tailoff the thrust unbalance between the SRM's caused a yaw transient that significantly delayed the staging time. For the 45° - 135° TVC actuator configuration, adverse roll-yaw torque from the remaining thrusting actuator precluded successful compensation; but for the 0° - 90° TVC configuration, compensation permitted some reduction of the delay in staging.

It is recommended that the 0° - 90° TVC actuator configuration be retained as a viable alternative to the baseline 45° - 135° TVC configuration and that additional studies be performed on staging compensation. It is also recommended that load relief studies be initiated to develop techniques for decreasing the effect of actuator failures and winds on vehicle loads during boost.

<u>DESIGN CONDITIONS</u>		SRM WITH HIGH THRUST	SRM WITH FAILED ACTUATOR	ACTUATOR FAILED	WIND
45° - 135° BASELINE ACTUATOR CONFIGURATION	MID-BOOST	LEEWARD	WINDWARD	LEFT	RIGHT CROSS
	TAILOFF	WINDWARD	WINDWARD	RIGHT	LEFT CROSS
				LEFT	RIGHT CROSS
	RIGHT	LEFT CROSS			
0° - 90° ACTUATOR CONFIGURATION	MID-BOOST	LEEWARD	WINDWARD	PITCH	CROSSWIND
	TAILOFF	WINDWARD	WINDWARD	YAW	CROSSWIND

- ACTUATOR FAILURES AT LIFTOFF PRODUCE LARGEST PERTURBATIONS.

FIGURE 1 DESIGN CONDITIONS

2.3 SIMULATION CALIBRATION

Using configuration and trajectory data obtained from Rockwell International, comparison trajectories were run in an attempt to verify JSC simulator results with those of Rockwell International. Results indicate that the trajectory obtained was in fairly good agreement with Rockwell International, however larger actuator deflections were noted and a larger Q-B was observed with the JSC simulator. It is suggested that the control system and control gains of the JSC simulator be checked for compatibility with the Rockwell International system. Results of this study are reported in Boeing Memorandum 5-2581-HOU-155, dated June 28, 1974.

3.0 STABILITY ANALYSIS

3.1 SUMMARY

The Space Shuttle Stability Analysis task included development and check-out of a sampled data stability analysis program for use in the analysis. This program is described in Section 3.2 with details in Volume IV of this report. Equations of motion were derived for use in the computer program and they are described in Sections 3.3 and 3.4.

Rigid body stability (one slosh mode included) analysis was performed for both pitch and lateral axes with results presented in Section 3.5. Effect of bending and slosh to bending - bending to slosh coupling on vehicle stability were investigated and reported in Section 3.6.

Actuator equations to represent +"Dog Wags Tail (DWT)" effect on the vehicle were derived. Stability margins with DWT terms in the equations were obtained; transfer functions of the DWT terms and DWT stability margins are reported in Section 3.7.

Space Shuttle vehicle is rigid body stable at all time points. Addition of bending terms produces instability, coupling terms provide slight stability improvement and DWT provides more stability relief. Addition of the selected filters stabilizes bending but is destabilizing to slosh; however, optimization of filters was not attempted during this analysis.

3.2 SAMPLED DATA STABILITY ANALYSIS PROGRAM

The Sampled Data Stability Analysis Program (SADSAP), formerly known as The Boeing-Huntsville Program BHA-369, was converted to the SBU 1110 EXEC 8 system. This program is a general purpose sampled data stability analysis program capable of providing frequency response and root locus data. The continuous system open loop and closed loop poles along with open loop zeros are also provided.

SADSAP computes R domain open loop frequency response and Z domain gain and phase root locus of a sampled data closed loop control system. The control system definition includes the S-domain characteristic matrix, sampling device location, sample period, optional zero order hold circuit, and optional transport lag. Output features of the program are Nichols plots, digital print of the frequency response and root locus analysis, and digital print of the partial fraction expansion of the open loop transfer function in the Z domain and R domain.

A detailed description of the SADSAP computer program is provided in Volume IV of this report. Input requirements are specified in Section 2.0, a discussion of technical methods in Section 3.0, flow charts in Section 4.0, a sample problem in Section 5.0, and a complete program listing in Section 6.0.

3.3 SPACE SHUTTLE PITCH AXES EQUATION OF MOTION

3.3.1 Introduction

Equations of motion suitable for inclusion in the Sampled Data Stability Analysis Program (SADSAP) were developed and are presented in Section 3.3.2 with a definition of symbols. This set of equations was developed specifically to determine the stability margin for the pitch plane vehicle and control systems, and to evaluate the effects of "Dog Wags Tail" and bending on stability. These are trajectory referenced perturbation equations, simplified by having those items removed that are negligible and by using small angle approximation. Sign conventions are the same as those discussed in the following reference:

Rockwell's Memorandum SD 73-SH-0097A, "Space Shuttle Guidance and Control Data Book," dated July 13, 1973.

Symbols are defined in Section 3.3.3. A matrix representation of the equations is shown in Section 3.3.4. The matrix may be expanded and other terms added as required by design iteration. The matrix representation was used in the stability analysis of Section 3.5.1.

3.3.2 Equations of Motion - Pitch (XZ Plane)

Rigid Rotation

$$\begin{aligned}
 I_Y \ddot{\theta} &= C_{m\alpha} q A \bar{c} \dot{\theta} - \frac{q A \bar{c} C_{m\alpha} \dot{Z}}{V} + q A C_{z\alpha} (X_{cg} - X_{AR}) \dot{\theta} \\
 &- \frac{q A C_{z\alpha} (X_{cg} - X_{AR}) \dot{Z}}{V} - q A C_{x\alpha} (Z_{cg} - Z_{AR}) \dot{\theta} + \frac{q A C_{x\alpha} (Z_{cg} - Z_{AR}) \dot{Z}}{V} \\
 &- \sum_{i=1}^5 \left[F_{Ei} (X_{cg} - X_{Ei}) + S_{Ei} K_3 \right] \delta_{E\theta i} - \sum_{i=1}^5 \left[(X_{cg} - X_{Ei}) S_{Ei} + I_{Ei} \right] \delta_{E\theta i} S^2 \\
 &+ \sum_{j=1}^2 m_{sj} \left[l_{sj} S^2 + \frac{(F-D)}{m} \right] Z_{sj}
 \end{aligned}$$

Rigid Translation

$$\begin{aligned}
 \ddot{Z} &= \ddot{y} + l_y \ddot{\theta} + \frac{F-D}{m} \theta \\
 \ddot{y} &= \frac{q A C_{z\alpha} \alpha}{m} - l_y \ddot{\theta} + \frac{F_{Ei} \delta_{E\theta i}}{m} + \sum_{i=1}^5 \frac{S_{Ei} \ddot{\theta}_{E\theta i}}{m} \\
 &- \sum_{j=1}^2 \frac{l_{sj}}{m} \ddot{Z}_{sj}
 \end{aligned}$$

Angular Relationship

$$\alpha = \theta - \frac{\dot{Z}}{V}$$

Bending (N Equations)

$$\begin{aligned}
 (S^2 + 2 \sum_{BK} \omega_{BK} S + \omega_{BK}^2) M_{BK} n_K &= \sum_{i=1}^5 F_{Ei} Z_{BEiK} \delta_{E\theta i} + \sum_{i=1}^5 \left(S_{Ei} Z_{BEiK} - I_{Ei} Z'_{BEiK} \right) \ddot{\theta}_{E\theta i} - \sum_{j=1}^2 [m_{sj} Z_{BjK} S^2 \\
 &- m_{sj} \frac{F-D}{m} Z'_{BjK}] Z_{sj} + C_{z\alpha} AR \alpha
 \end{aligned}$$

Slosh Equations (2)

$$[S^2 + 2 \sum_{sj} \omega_{sj} S + \omega_{sj}^2] Z_{sj} = -\ddot{Z} + l_{sj} \ddot{\theta} + \frac{F-D}{m} \theta - \sum_{k=1}^N \left[Z_{BsJK} S^2 - \left(\frac{F-D}{m} \right) Z'_{BsJK} \right] n_K$$

3.3.2 Equations of Motion - Pitch (XZ Plane) (Continued)

Sensed Attitude

$$\theta_T = \theta + \sum_{K=1}^N Z'_{B PK} \eta_K$$

Sensed Attitude Rate

$$\dot{\theta}_T = \dot{\theta} + \sum_{K=1}^N Z'_{BRGK} \dot{\eta}_K$$

Sensed Acceleration

$$\ddot{\theta}_T = \ddot{\theta} + \sum_{K=1}^N Z'_{BYK} \ddot{\eta}_K$$

Control Equation

$$\delta_{C\theta} = A_{0\theta} F_{\theta} F_P \theta_T + A_{1\theta} F_{\theta} F_{RG} \dot{\theta}_T + g_2 F_Y F_A \ddot{\theta}_T$$

Actuator Equations (5)

$$\delta_{\theta i} = W_{ss} \delta_{C\theta i} + W_{fs} \delta_{ERi}$$

$$\delta_{ERi} = \sum_{k=1}^i \frac{z_{ei} m_{ei}}{z_{ai}} [Z_{BEiK} - Z'_{BEiK} z_e] \ddot{\eta}_k$$

3.3.3 Definition of Symbols - Pitch (XZ Plane)

Symbol	Units	Description
θ	rad	Attitude error angle of undeformed vehicle in the XZ plane
\ddot{y}	m/sec ²	Acceleration of rigid vehicle at accelerometer location
η_K	m	Bending displacement of Kth mode
Z_{sj}	m	Sloshing fluid displacement in the Jth tank
$\delta_{C\theta i}$	rad	Pitch commanded engine angle for the ith engine
\ddot{z}	m/sec ²	Acceleration in the Z direction of the CG
α	rad	Pitch angle of attack
$\delta_{\theta i}$	rad	Engine angle of the ith engine
θ_T	rad	Attitude error angle at inertial platform
$\dot{\theta}_T$	rad/sec	Angular velocity at rate gyro location
\ddot{y}_T	m/sec ²	Lateral acceleration at accelerometer location
<u>Calculated Data</u>		
C_1	1/sec ²	$\frac{qA\bar{c}}{I_y} C_{m\alpha}$
C_2	1/sec ²	$\frac{qAC_{z\alpha}(X_{cg} - X_{AR})}{I_y}$
C_3	$\frac{1}{\text{sec}^2}$	$\frac{qAC_{x\alpha}(Z_{cg} - Z_{AR})}{I_y}$
C_4	$\frac{m}{\text{sec}^2}$	$\frac{qA}{m} C_{z\alpha}$

3.3.3 Definition of Symbols - Pitch (XZ Plane) (Continued)

Symbol	Units	Description
K_3	m/sec^2	$\frac{F-D}{m}$
C_{Ei}	Newton meters	$F_{Ei} (X_{cg} - X_{Ei}) + S_{Ei} K_3$
TWD_i	$kg-m^2$	$S_{Ei} (X_{cg} - X_{Ei}) + I_{Ei}$
KB_{0iK}	m	$\frac{S_{Ei} Z_{EiK} - I_{Ei} Z'_{EiK}}{M_{BK}}$
K_{2j}	$kg-m$	$M_{sj} l_{sj}$
K_{0j}	Newtons	$\frac{M_{sj}}{m} (F-D)$
K_{E0iK}	m/sec^2	$\frac{F_{Ei} Z_{EiK}}{M_{BK}}$
K_{00jK}	$1/sec^2$	$\frac{F-D}{m} \frac{M_{sj}}{M_{BK}} Z'_{jK}$
K_{20jk}	--	$\frac{M_{sj}}{M_{BK}} Z_{jK}$
l_{sj}	m	Distance from cg to Slosh attach point ($X_{cg} - X_{sj}$)
l_y	m	Distance from cg to accelerometer ($X_{cg} - X_y$)
l_{ei}	m	Distance from ith engine Cg to Gimbal ($X_{Ei} - X_{Ecgi}$)
l_a	m	Moment arm of the actuators

3.3.3 Definition of Symbols - Pitch (XZ Plane) (Continued)

Vehicle Data

Symbol	Units	Description
$C_{m\alpha}$	1/rad	Derivative of moment about Y axes with respect to α
$C_{Z\alpha}$	1/rad	Derivative of pitch lift coefficient with respect to α
$C_{X\alpha}$	1/rad	Derivative of pitch drag coefficient with respect to α
q	Newton/m ²	Dynamic pressure
A	m ²	Wing surface area
\bar{c}	m	Length of mean aerodynamic chord
I_y	kg-m ²	Moment of inertia about the Y axis
v	m/sec	Forward velocity
F_{Ei}	Newtons	Thrust of the ith engine
S_{Ei}	kg-m	ith engine first moment about gimbal
I_{Ei}	kg-m ²	ith engine 2nd moment about gimbal
m_{sj}	kg	Slosh mass jth tank
F	Newton	Total thrust (all engines)
D	Newton	Longitudinal drag force
m	kg	Vehicle mass
ζ_{BK}	-	Damping factor kth bending mode
S		Laplace transfer variable
ω_{BK}	rad/sec	Bending mode natural frequency kth bending mode
M_{BK}	kg	Generalized mass kth bending mode
Z_{BEiK}	-	kth bending mode shape at gimbal of ith engine

3.3.3 Definition of Symbols - Pitch (XZ Plane) (Continued)

Symbol	Units	Description
Z'_{BEiK}	rad/m	kth bending mode slope at gimbal of ith engine
Z_{ARK}	-	kth bending mode shape at aerodynamic reference point
ζ_{sj}	-	Slosh damping factor jth tank
ω_{sj}	rad/sec	Slosh natural frequency, jth tank
Z_{Bsjk}	-	kth bending mode shape at jth tank
Z'_{Bsjk}	rad/sec	kth bending mode slope at jth tank
Z'_{BPK}	rad/sec	kth bending mode slope at platform location
Z'_{BRGK}	rad/sec	kth bending mode slope at rate gyro location
Z_{BYK}	-	kth bending mode shape at accelerometer locations
A_{00}	-	Pitch attitude control gain
A_{10}	sec	Pitch attitude rate control gain
g_{20}	rad-sec ² /m	Pitch acceleration control gain
F_{θ}		Attitude filter transfer function
$F_{\dot{\theta}}$		Attitude rate filter transfer function
F_{γ}		Acceleration filter transfer function
F_p		Platform transfer function
F_{RG}		Rate gyro transfer function
F_A		Accelerometer transfer function
W_{fs}	rad/Newton	Engine actuator transfer function Ratio of $\delta_{\theta i}$ to external force on engine
W_{ss}		Engine actuator transfer function
X_{cg}, Z_{cg}	m	Center of gravity along the X,Z axis

3.3.3 Definition of Symbols - Pitch (XZ Plane) (Continued)

Symbol	Units	Description
X_{sj}, Z_{sj}	m	Slosh mass location along the X,Z axes
X_{AR}, Z_{AR}	m	Aerodynamic reference point along the X,Z axes
X_Y, Z_Y	m	Accelerometer location along the X,Z axes
X_{Ei}, Z_{Ei}	m	Engine gimbal location along the X,Z axes
ω_{RG}	rad/sec	Rate gyro natural frequency
ω_a	rad/sec	Accelerometer natural frequency
ω_p	rad/sec	Platform natural frequency
ζ_{RG}	-	Rate gyro damping factor
ζ_Y	-	Accelerometer damping factor
ζ_p	-	Platform damping factor

3.3.4 Matrix Representation - Pitch (XZ Plane)

$$\begin{aligned}
 & (S^2 - C_1 - C_2 - C_3) \theta + (C_1/r + C_2/r + C_3/r) Z S - \frac{1}{I_y} \sum_{j=1}^2 (K_{0j} + K_{2j} S^2) Z_{sj} \\
 & + \frac{1}{I_y} \sum_{i=1}^5 (C_{Ei} + TWD_i S^2) \delta_{\theta i} = 0 \\
 & (C_4 + K_3) \theta - (S + C_4/r) Z - \sum_{j=1}^2 \frac{M_{sj}}{m} S^2 Z_{sj} + \frac{1}{m} \sum_{i=1}^5 (F_{Ei} + S_{Ei} S^2) \delta_{\theta i} = 0 \\
 & -(S^2 \epsilon_{sj} + K_3) \theta + Z S^2 + (S^2 + 2\zeta_{sj} \omega_{sj} S + \omega_{sj}^2) Z_{sj} + \sum_{k=1}^N (Z_{\omega jk} S^2 - K_3 Z'_{Bsj}) \eta_k = 0 \\
 & (K_{2\theta jk} S^2 - K_{0\theta jk}) Z_{sj} - (K_{E\theta i k} + K_{B\theta i k} S^2) \delta_{\theta i} + (S^2 + 2\zeta_{BK} \omega_{BK} S + \omega_{BK}^2) \eta_k = 0 \\
 & \delta_{\theta i} - \frac{N_{ssi}}{D_{ssi}} \delta_{c\theta i} - \frac{N_{fsi}}{D_{fsi}} \delta_{ERi} = 0 \\
 & \frac{A_0 N_{\theta p} N_{\theta p}}{D_{\theta p}} \dot{\theta}_T + \frac{A_1 N_{\theta RG}}{D_{\theta RG}} \ddot{\theta}_T + \frac{g_2 N_{\gamma A}}{D_{\gamma A}} \ddot{\gamma} - \delta_{c\theta i} = 0 \\
 & -\theta - Z'_{BPK} \eta_k + \theta_T = 0 \\
 & -\theta S - Z'_{BPK} S \eta_k + \theta_T S = 0 \\
 & (K_3 + \epsilon_{\gamma} S^2) \theta - Z S^2 - Z_{Byk} S^2 \eta_k + \gamma S^2 = 0
 \end{aligned}$$

3.4 SPACE SHUTTLE LATERAL AXES EQUATION OF MOTION

3.4.1 Introduction

Lateral axes equations of motion are presented in Section 3.4.2 with a definition of symbols. The defined equations of motion are suitable for inclusion in the Sampled Data Stability Analysis Program (SADSAP). This set of equations was developed specifically to determine the stability margins for the lateral axes vehicle and control systems. Trajectory referenced perturbation equations are simplified by the removal of negligible effect terms and the pitch axes cross coupling terms. Further simplification is made by limiting the perturbations to small angles which is acceptable for point time stability analysis. Sign conventions are the same as those discussed in the following reference.

Dockwell Memorandum SD73-SH0097A, "Space Shuttle
Guidance and Control Data Book," dated July 13, 1973.

Symbols are defined in Section 3.4.3. The equations are rewritten in a form suitable for inclusion in matrix format in Section 3.4.4.

Expansion of the equations to include the terms neglected needs to be investigated; especially such terms as "Dog Wags Tail" and aerodynamic damping. Bending equations may require expansion to account for the slosh and engine representation in the structural dynamic analysis.

3.4.2 Equations of Motion - (Lateral Axes)

Yaw Rotation

$$\begin{aligned} \psi S^2 = & -\left(\frac{qAb}{I_z} C_{n\beta}\right) \psi + \frac{qA}{I_z} (X_{cg} - X_{AR}) C_{y\beta} \psi + \frac{qAb^2}{2I_z V} C_{nr} \psi S + \frac{qAb}{I_z} \frac{C_{n\beta}}{V} Y S \\ & - \frac{qA}{I_z} \frac{(X_{cg} - X_{AR})}{V} C_{y\beta} Y S - \frac{qAb}{2I_z V} (X_{cg} - X_{AR}) C_{yp} \phi S + \frac{qAb^2}{2I_z V} C_{np} \phi S \\ & + \frac{qAb}{2I_z V} (X_{cg} - X_{AR}) C_{yr} \psi S + \frac{qAb}{I_z} C_{n\delta r} \delta_r - \frac{qA}{I_z} C_{y\delta r} (X_{cg} - X_{AR}) \delta_r \\ & - \frac{1}{I_z} \sum_{i=1}^5 [F_{Ei} (X_{cg} - X_{Ei}) + (S_{Ei} [X_{cg} - X_{Ei}] + I_{Ei}) S^2] \delta_{\psi i} \\ & + \frac{1}{I_z} \sum_{j=1}^2 [m_{sj} l_{xsj} S^2 + m_{sj} \frac{F-D}{m}] Y_{sj} \end{aligned}$$

Yaw Translation

$$\begin{aligned} Y S^2 = & \frac{qA C_{y\beta}}{mV} Y S - \frac{qA}{m} C_{y\beta} \psi + \frac{F-D}{m} \psi + \frac{qAb}{2Vm} C_{yr} \psi S + \frac{qAb}{2Vm} C_{yp} \phi S + \frac{qA}{m} C_{y\delta r} \delta_r + \\ & \frac{1}{m} \sum_{i=1}^5 (F_{Ei} + S_{Ei} S^2) \delta_{\psi i} - \sum_{j=1}^2 \frac{m_{sj}}{m} Y_{sj} S^2 \end{aligned}$$

Lateral Acceleration

$$Y S^2 = -\psi S^2 \ddot{y}_x - \phi S^2 \ddot{y}_z + Y S^2 - \frac{F-D}{m} \psi$$

3.4.2 Equations of Motion - (Lateral Axes) (Continued)

Roll Rotation

$$\phi S^2 = \frac{qAb^2}{2I_x V} C_{1p} \phi S + \frac{qAb}{I_x 2V} C_{yp} (Z_{cg} - Z_{AR}) \phi S - \frac{qAb}{I_x} C_{1\beta} \psi + \frac{qAb^2}{I_x 2V} C_{1r} \psi S -$$

$$\frac{qA}{I_x} C_{y\beta} (Z_{cg} - Z_{AR}) \psi + \frac{qA}{I_x} \frac{C_{1\beta}}{V} YS + \frac{qA}{I_x V} C_{y\beta} (Z_{cg} - Z_{AR}) YS + \frac{qAb}{I_x 2V} C_{yr} (Z_{cg} - Z_{AR}) \psi S$$

$$+ \frac{qA}{I_x} C_{y\delta r} (Z_{cg} - Z_{AR}) \delta_r + \frac{qAb}{I_x} C_{1\delta r} \delta_r - \frac{1}{I_x} \sum_{i=2}^5 [F_{Ei} + S_{Ei} S^2] d_{YEi} \delta_{\phi i} -$$

$$\frac{1}{I_x} \sum_{i=1}^5 (F_{Ei} + S_{Ei} S^2) (Z_{cg} - Z_{Ej}) \delta_{\psi i} + \frac{1}{I_x} \sum_{j=1}^2 m_{sj} l_{zsj} S^2 Y_{sj}$$

Yaw Slosh Equations (j=1,2)

$$[S^2 + 2\zeta_{sj} \omega_{sj} S + \omega_{sj}^2] Y_{sj} = YS^2 + (l_{xsj} S^2 + \frac{F-D}{m}) \psi - l_{zsj} \phi S^2 - \sum_{k=1}^N [Y_{sjk} S^2 -$$

$$\frac{F-D}{m} Y'_{sjk}] \eta_k$$

Yaw Bending Equations (k=1,2, ...N)

$$(S^2 + 2\zeta_{BK} \omega_{BK} S + \omega_{BK}^2) m_{BK} \eta_k = \sum_{i=1}^5 F_{Ei} Y_{BEik} \delta_{\psi i} + \sum_{i=1}^5 (S_{Ei} Y_{BEik} - I_{Ei} Y'_{BEik}) \delta_{\psi i} S^2 +$$

$$qA C_{y\beta} Y_{ARK} \beta - \sum_{j=1}^2 m_{sj} (Y_{sjk} S^2 - \frac{F-D}{m} Y'_{sjk}) Y_{sj}$$

3.4.2 Equations of Motion - (Lateral Axes) (Continued)

Torsion Equations (k=1,2,3, ...N)

$$(S^2 + 2\zeta_{\tau k} \omega_{\tau k} S + \omega_{\tau k}^2) \eta_{\tau k} J_k = \sum_{i=2}^5 [F_{Ei} + S_{Ei} S^2] d_{YEi} \tau_{Eik} \delta_{\phi i} +$$

$$\sum_{i=1}^5 (F_{Ei} + S_{Ei} S^2) (Z_{cg} - Z_{Ei}) \tau_{Eik} \delta_{\psi i} - \sum_{j=1}^2 M_{sj} (S^2 - \frac{F-D}{M}) Z_{sj} \tau_{sjk} Y_{sj}$$

$$+ qA_{\tau ARk} (Z_{cg} - Z_{AR}) [C_{yB} \frac{YS}{V} - \psi] + \frac{b}{2V} C_{yp} \phi S + C_{y\delta r} \delta_r]$$

Sensed Attitude

$$\psi_T = \psi + \sum_{k=1}^N Y'_{Bpk} \eta_k$$

$$\phi_T = \phi - \sum_{k=1}^n \tau_{pk} \eta_{\tau k}$$

Sensed Attitude Rate

$$\psi_T S = \psi S + \sum_{k=1}^N Y_{BRGk} \eta_k S$$

$$\phi_T S = \phi S - \sum_{k=1}^N \tau_{RGk} \eta_{\tau k} S$$

Sensed Acceleration

$$\gamma_T S^2 = \gamma S^2 + \sum_{k=1}^N Y_{Byk} \eta_k S^2$$

Control Equations

$$\delta_{\psi} = \sum_{N=0}^p a_{N\psi} F_{N\psi} S_{N\psi} V_{N\psi}$$

$$\delta_{\phi} = \sum_{N=0}^q a_{N\phi} F_{N\phi} S_{N\phi} V_{N\phi}$$

3.4.2 Equations of Motion - (Lateral Axes) (Continued)

Engine Equations (5)

$$\delta_{\psi 1} = -2K_{TSS} \delta_{\phi}$$

$$\delta_{\psi 2} = \delta_{\psi 3} = 2K_{TSS} \delta_{\psi}$$

$$\delta_{\psi 4} = \delta_{\psi 5} = K_{TSS} \delta_{\psi}$$

$$\delta_{\phi 1} = -2K_{TSS} \delta_{\phi}$$

$$\delta_{\phi 2} = -\delta_{\phi 3} = -K_{TSS} \delta_{\phi}$$

$$\delta_{\phi 4} = -\delta_{\phi 5} = -K_{TSS} \delta_{\phi}$$

Rudder Equations

$$\delta_r = -5K_{TRR} \delta_{\phi}$$

3.4.3 Definition of Symbols - (Lateral Axes)

Symbol	Units	Description
Variables		
ϕ, ψ	rad	Attitude error angle of undeformed vehicle in the yaw and roll axes
\ddot{Y}	m/sec ²	Acceleration of rigid vehicle at accelerometer location
n_k	m	Bending displacement of kth mode
$n_{\tau k}$	rad	Torsional displacement of the kth mode
Y_{sj}	m	Sloshing fluid displacement in the jth tank
δ_ϕ	rad	Roll engine command signal
$\delta_{\phi ci}$	rad	Roll commanded engine angle for the ith engine
δ_ψ	rad	Yaw engine command signal
$\delta_{\psi ci}$	rad	Yaw commanded engine angle for the ith engine
\ddot{Y}	m/sec ²	Acceleration of the cg in the Y direction
β	rad	Side slip angle
$\delta_{\phi i}, \delta_{\psi i}$	rad	Roll, yaw engine angle of the ith engine
δ_{cr}	rad	Commanded rudder deflection angle
δ_r	rad	Rudder deflection angle
ϕ_T, ψ_T	rad	Roll, yaw attitude error angle at inertial platform
$\dot{\phi}_T, \dot{\psi}_T$	rad/sec	Roll, yaw angular velocity at rate gyro location
\ddot{Y}_T	m/sec	Lateral acceleration at accelerometer location

3.4.3 Definition of Symbols - (Lateral Axes) (Continued)

Symbol	Units	Description
Vehicle Data (Environment and Configuration)		
q	Newton/m ²	Dynamic pressure
A	m ²	Wing surface area
b	m	Wing span
X _{AR} , Z _{AR}	m	Aerodynamic reference point along the X, Z axes
D	Newtons	Longitudinal drag force
Vehicle Data (Mass and Trajectory)		
I _x , I _z	kg-m ²	Moment of inertia about the X, Z axes
V	m/sec	Forward velocity
m	kg	Vehicle mass
F	Newtons	Total thrust (all engines)
Vehicle Data (Engine)		
F _{Ei}	Newtons	Thrust of the ith engine
S _{Ei}	kg-m	ith engine first moment about gimbal
I _{Ei}	kg-m ²	ith engine 2nd moment about gimbal
X _{Ei} , Y _{Ei} , Z _{Ei}	m	ith engine gimbal location along the X, Y, Z axes
d _{YEi} , d _{ZEi}	m	Distance from cg to ith engine along X,Z axes.
Vehicle Data (Slosh)		
ζ _{sj}	-	Slosh damping factor, jth tank
ω _{sj}	rad/sec	Slosh natural frequency, jth tank
m _{sj}	kg	Slosh mass, jth tank
X _{saj} , Y _{saj} , Z _{saj}	m	Slosh mass location along the X, Y, Z axes

3.4.3 Definition of Symbols - (Lateral Axes) (Continued)

Symbol	Units	Description
Vehicle Data (Bending)		
ζ_{BK}	-	Damping factor kth bending mode
ω_{BK}	rad/sec	Bending mode natural frequency kth bending mode
m_{BK}	kg	Generalized mass kth bending mode
Y_{BEiK}	-	kth bending mode shape at gimbal of ith engine
Y'_{BEiK}	rad/M	kth bending mode slope at gimbal of ith engine
Y_{ARK}	-	kth bending mode shape at aerodynamic reference point
Y_{Bsjk}	-	kth bending mode shape at jth tank
Y'_{Bsjk}	rad/M	kth bending mode slope at jth tank
Y'_{BPK}	rad/M	kth bending mode slope at platform location
Y'_{BRGK}	rad/M	kth bending mode slope at rate gyro location
Y_{BYK}	-	kth bending mode shape at accelerometer location
ζ_{TK}	-	Damping factor kth torsional mode
ω_{TK}	rad/sec	kth torsional mode natural frequency
J_K	$k-m^2$	Generalized moment of inertia, kth torsional mode
T_{EiK}	-	Kth torsional mode shape at gimbal of ith engine
T_{SJK}	-	Kth torsional mode shape at jth slosh attach point
T_{ARK}	-	Kth torsional mode shape at aerodynamic reference point
T_{pk}	-	Kth torsional mode shape at platform
T_{RGK}	-	Kth torsional mode shape at rate gyro

3.4.3 Definition of Symbols - (Lateral Axes) (Continued)

Symbol	Units	Description
Vehicle Data (Sensor, Control System & TVC)		
$A_{0\phi} A_{0\psi}$	-	Roll and yaw attitude control gains
$A_{1\phi} A_{1\psi}$	sec	Roll and yaw attitude rate control gains
$g_{2\phi} g_{2\psi}$	rad-sec ² /m	Roll and yaw acceleration control gains
$F_{\phi} F_{\psi}$	-	Roll and yaw attitude filter transfer functions
$F_{\dot{\phi}} F_{\dot{\psi}}$	-	Roll and yaw attitude rate filter transfer functions
$F_{\ddot{Y}}$	-	Acceleration filter transfer function
F_p	-	Platform transfer function
F_{RG}	-	Rate gyro transfer function
F_A	-	Accelerometer transfer function
W_{SS}	-	Engine actuator transfer function
W_{RR}	-	Rudder actuator transfer function
$X_{cg} Y_{cg} Z_{cg}$	m	Center of gravity along the X,Y,Z axes
$X_{Y Y} Y_{Y Y} Z_{Y Y}$	m	Accelerometer location along the X,Y,Z axes
ω_{RG}	rad/sec	Rate gyro natural frequency
$\omega_{\ddot{Y}}$	rad/sec	Accelerometer natural frequency
ω_p	rad/sec	Platform natural frequency
ζ_{RG}	-	Rate gyro damping factor
$\zeta_{\ddot{Y}}$	-	Accelerometer damping factor
ζ_p	-	Platform damping factor
S	1/sec	Laplace transform variable

3.4.3 Definition of Symbols - (Lateral Axes) (Continued)

Symbol	Units	Description
Vehicle Data (Aerodynamics)		
$C_{n\beta}$	1/rad	Moment coefficient about Z axes with respect to β
$C_{n\dot{\phi}}$	1/rad	Moment coefficient about Z axes with respect to $\dot{\phi}$
C_{nr}	1/rad	Moment coefficient about Z axes with respect to $\dot{\psi}$
$C_{n\delta r}$	1/rad	Moment coefficient about Z axes with respect to δr
$C_{y\beta}$	1/rad	Aerodynamic force coefficient along Y axes with respect to β
$C_{y\dot{\phi}}$	1/rad	Aerodynamic force coefficient along Y axes with respect to $\dot{\phi}$
C_{yr}	1/rad	Aerodynamic force coefficient along Y axes with respect to $\dot{\psi}$
$C_{y\delta r}$	1/rad	Aerodynamic force coefficient along Y axes with respect to δr
$C_{l\beta}$	1/rad	Moment coefficient about X axes with respect to β
$C_{l\dot{\phi}}$	1/rad	Moment coefficient about X axes with respect to $\dot{\phi}$
C_{lr}	1/rad	Moment coefficient about X axes with respect to $\dot{\psi}$
$C_{l\delta r}$	1/rad	Moment coefficient about X axes with respect to δr

3.4.3 Definition of Symbols - (Lateral Axes) (Continued)

Symbol	Units	Description
Vehicle Data (Calculated Constants)		
$C_{5\beta}$	$1/\text{sec}^2$	$\frac{qAb}{I_z} C_{n\beta}$
C_{5p}	$1/\text{sec}$	$\frac{qAb^2}{2I_z V} C_{np}$
C_{5r}	$1/\text{sec}$	$\frac{qAb^2}{2I_z V} C_{nr}$
$C_{5\delta r}$	$1/\text{sec}^2$	$\frac{qAb}{I_z} C_{n\delta r}$
$C_{6\beta}$	$1/\text{sec}^2$	$\frac{qA}{I_z} (X_{cg} - X_{AR}) C_{y\beta}$
C_{6p}	$1/\text{sec}$	$\frac{qAb}{2I_z V} (X_{cg} - X_{AR}) C_{yp}$
C_{6r}	$1/\text{sec}$	$\frac{qAb}{2I_z V} (X_{cg} - X_{AR}) C_{yr}$
$C_{6\delta r}$	$1/\text{sec}^2$	$\frac{qA}{I_z} (X_{cg} - X_{AR}) C_{y\delta r}$
$C_{7\beta}$	$1/\text{sec}^2$	$\frac{qA}{I_x} (Z_{cg} - Z_{AR}) C_{y\beta}$
C_{7p}	$1/\text{sec}$	$\frac{qAb}{2I_x V} (Z_{cg} - Z_{AR}) C_{yp}$
C_{7r}	$1/\text{sec}$	$\frac{qAb}{2I_x V} (Z_{cg} - Z_{AR}) C_{yr}$
$C_{7\delta r}$	$1/\text{sec}^2$	$\frac{qA}{I_x} (Z_{cg} - Z_{AR}) C_{y\delta r}$
$C_{8\beta}$	m/sec^2	$\frac{qA}{m} C_{y\beta}$
C_{8p}	m/sec	$\frac{qAb}{2mv} C_{yp}$
C_{8r}	m/sec	$\frac{qAb}{2mv} C_{yr}$
$C_{8\delta r}$	m/sec^2	$\frac{qA}{m} C_{y\delta r}$

3.4.3 Definition of Symbols - (Lateral Axes) (Continued)

Symbol	Units	Description
Vehicle Data (Calculated Constants)		
$C_{g\beta}$	$1/\text{sec}^2$	$\frac{qAb}{I_x} C_{1\beta}$
C_{gp}	$1/\text{sec}$	$\frac{qAb^2}{2VI_x} C_{1p}$
C_{gr}	$1/\text{sec}$	$\frac{qAb^2}{2VI_x} C_{1r}$
$C_{g\delta r}$	$1/\text{sec}^2$	$\frac{qAb}{I_x} C_{1\delta r}$
C_{Ei}	Newton-M	$F_{Ei} (X_{cg} - X_{Ei})$
TWD_i	kg-m^2	$S_{Ei} (X_{cg} - X_{Ei}) + I_{Ei}$
K_3	m/sec^2	$\frac{F - D}{m}$
$KE\phi_{jk}$	$1/\text{m-sec}^2$	$\frac{F_{Ei} \tau_{Eik}}{J_k}$
$KB\phi_{jk}$	$1/\text{m}$	$\frac{S_{Ei} \tau_{Eik}}{J_k}$
$KE\psi_{jk}$	m/sec^2	$\frac{F_{Ei} Y_{BEik}}{m_{Bk}}$
$KB\psi_{jk}$	m	$\frac{S_{Ei} Y_{BEik} - I_{Ei} Y'_{BEik}}{m_{Bk}}$
K_{0j}	Newtons	$M_{sj} K_3$
K_{2j}	kg-m	$M_{sj} l_{xsj}$
$K_{0\psi_{jk}}$	$1/\text{sec}^2$	$\frac{K_3 Y'_{sjk} m_{sj}}{m_{Bk}}$
$K_{2\psi_{jk}}$	-	$\frac{m_{sj} Y_{sjk}}{m_{Bk}}$

3.4.3 Definition of Symbols - (Lateral Axes) (Continued)

Symbol	Units	Description
Vehicle Data (Calculated Constants)		
l_{xsj}	m	Distance from cg to s'losh attach point ($X_{cg} - X_{saj}$) along the X axes
l_{zsj}	m	Distance from cg to s'losh attach point ($Z_{cg} - Z_{saj}$) along the Z axes
$l_{\gamma x}$	m	Distance from cg to accelerometer ($X_{cg} - X_{\gamma}$)
$l_{\gamma z}$	m	Distance from cg to accelerometer ($Z_{cg} - Z_{\gamma}$)

3.4.4 Matrix Representation - (Lateral Axes)

Rewriting the sets of equations for use in a matrix, we have:

$$(S^2 - C_{5r}S - C_{6r}S + C_{5\beta} - C_{6\beta})\psi - \frac{(C_{5\beta} - C_{6\beta})YS}{V} + (C_{6p} - C_{5p})\phi S - (C_{5\delta r} - C_{6\delta r})\delta_r + \frac{1}{I_z} \sum_{i=1}^5 (C_{Ei} + TWD_i S^2) \delta_{\psi i} - \frac{1}{I_z} \sum_{j=1}^2 (K_{2j} S^2 + K_{0j}) Y_{sj} = 0 \quad (1)$$

$$(-C_{8r}S + C_{8\beta} - K_3)\psi + (S^2 - \frac{C_{8\beta}S}{V})Y - C_{8p}\phi S - C_{8\epsilon r}\delta_r - \frac{1}{m} \sum_{i=1}^5 (F_{Ei} + S_{Ei} S^2) \delta_{\psi i} +$$

$$\sum_{j=1}^2 \frac{m_{sj}}{m} Y_{sj} S^2 = 0 \quad (2)$$

$$(I_{\dot{y}x} S^2 + K_3)\psi - S^2 Y + S^2 I_{\dot{y}z} \phi + S^2 Y = 0 \quad (3)$$

$$(-C_{9r}S - C_{7r}S + C_{9\beta} + C_{7\beta})\psi - \frac{(C_{7\beta} + C_{9\beta})YS}{V} + (S^2 - C_{9p}S - C_{7p}S)\phi -$$

$$(C_{7\delta r} + C_{9\delta r})\delta_r + \frac{1}{I_y} \sum_{i=2}^5 [F_{Ei} + S_{Ei} S^2] d_{YEi} \delta_{\phi i} + \frac{1}{I_x} \sum_{i=1}^5 (F_{Ei} + S_{Ei} S^2) d_{ZEi} \delta_{\psi i} -$$

$$\frac{1}{I_x} \sum_{j=1}^2 m_{sj} I_{Zsj} S^2 Y_{sj} = 0 \quad (4)$$

$$-(I_{Xsj} S^2 + K_3)\psi - Y S^2 + I_{Zsj} \phi S^2 + (S^2 + 2\zeta_{sj} \omega_{sj} S + \omega_{sj}^2) Y_{sj} +$$

$$\sum_{k=1}^N [Y_{sjk} S^2 - K_3 Y'_{sjk}] r_k = 0 \quad (5)$$

$$- \frac{gA}{M_{Bk}} C_{Y\beta} Y_{ARk\beta} - \sum_{i=1}^5 (K_{E\psi ik} + K_{B\psi ik} S^2) \delta_{\psi i} + \sum_{j=1}^2 (K_{2\psi jk} S^2 - K_{0\psi jk}) Y_{sj} +$$

$$(S^2 + 2\zeta_{Bk} \omega_{Bk} S + \omega_{Bk}^2) r_k = 0 \quad (6)$$

3.4.4 Matrix Representation - (Lateral Axes) (Continued)

$$-\frac{gA}{j_k} \tau_{ARK} (Z_{cg} - Z_{AR}) [C_{Y\beta} (\frac{YS}{V} - \psi) + \frac{b}{2V} C_{yp} \phi S + C_{y\delta r} \delta_r] -$$

$$\sum_{i=1}^5 [KE\phi_{ik} + KB\phi_{ik} S^2] \frac{Z_{cg} - Z_{Ej}}{[Cg - Z_{Ej}]} \delta_{\psi i} - \sum_{i=2}^5 [KE\phi_{ik} + KB\phi_{ik} S^2] d_{YEi} \delta_{\phi i} +$$

$$\sum_{j=1}^2 \frac{m_{sj}}{j_k} [S^2 - K_3] l_{Zsj} \tau_{sjk} Y_{sj} + (S^2 + 2\zeta_{\tau k} \omega_{\tau k} S + \omega_{\tau k}^2) \eta_{\tau k} = 0 \quad (7)$$

$$-\psi - \sum_{k=1}^N Y' Bpk^n k + \psi_T = 0 \quad (8)$$

$$-\phi + \sum_{k=1}^N \tau_{pk} \eta_{\tau k} + \phi_T = 0 \quad (9)$$

$$-\psi S - \sum_{k=1}^N Y' BRG^n k S + \psi_T S = 0 \quad (10)$$

$$-\phi S + \sum_{k=1}^N \tau_{RGk} \eta_{\tau k} S + \phi_T S = 0 \quad (11)$$

$$-\gamma S^2 - \sum_{k=1}^N Y_{\gamma k} \eta_k S^2 + \gamma_T S^2 = 0 \quad (12)$$

$$\delta_{\psi} - \sum_{N=0}^p a_{N\psi} F_{N\psi} S_{N\psi} V_{N\psi} = 0 \quad (13)$$

$$\delta_{\phi} - \sum_{N=0}^q a_{N\phi} F_{N\phi} S_{N\phi} V_{N\phi} = 0 \quad (14)$$

$$\delta_{\psi 1} + 2k_{TSS} \delta_{\phi} = 0 \quad (15)$$

$$\delta_{\psi 2} - 2k_{TSS} \delta_{\psi} = 0 = \delta_{\psi 3} - 2k_{TSS} \delta_{\psi} \quad (16 \& 17)$$

$$\delta_{\psi 4} - (2)k_{TSS} \delta_{\psi} = 0 = \delta_{\psi 5} - (2)k_{TSS} \delta_{\psi} \quad (18 \& 19)$$

$$+ k_{TSS} \delta_{\phi} = 0 = \delta_{\psi 3} - k_{TSS} \delta_{\phi}$$

3.4.4 Matrix Representation - (Lateral Axes) (Continued)

$$\delta_{\phi 4} + k_{TSS} \delta_{\phi} = 0 = \delta_{\phi 5} - k_{TSS} \delta_{\phi} \quad (22 \text{ \& } 23)$$

$$\delta_r + 5k_{TRR} \delta_{\phi} = 0 \quad (24)$$

3.5 RIGID BODY STABILITY ANALYSIS

Frequency response data was obtained for each axes of the Space Shuttle Vehicle. This is a rigid body vehicle with one slosh mode. Stability margins are obtained by Nyquist analysis with the sampler at the commanded engine angle location. All vehicle data was taken from the following reference:

Rockwell Memorandum DS 73-SH-0097A, "Space Shuttle Guidance and Control Data Book" dated July 13, 1973.

3.5.1 Pitch Axes

Pitch axis frequency response data in Nichols plot format is shown in Figures 2 through 9. The minimum gain margin is 13.3db at SRM shutdown and the minimum phase margin is 42.6 degrees at SRM shutdown (Figure 4).

3.5.2 Yaw Axis

Stability margins are obtained with a closed loop roll system and the yaw system sampler at the commanded engine angle location. Yaw axis frequency response data in Nichols plot format is shown in Figures 10 through 17. The minimum gain margin is 0.55 db at max Q and minimum phase margin is 7.01 degrees at max Q (Figure 12).

3.5.3 Roll Axis

Stability margins are obtained with a closed loop yaw system and the roll system sampler at the commanded engine angle location. Roll axis frequency response data in Nichols plot format is shown in Figures 18 through 25. Minimum gain margin is 15.5 db at 70 seconds and minimum phase margin is 63 degrees at 70 seconds (Figure 21).

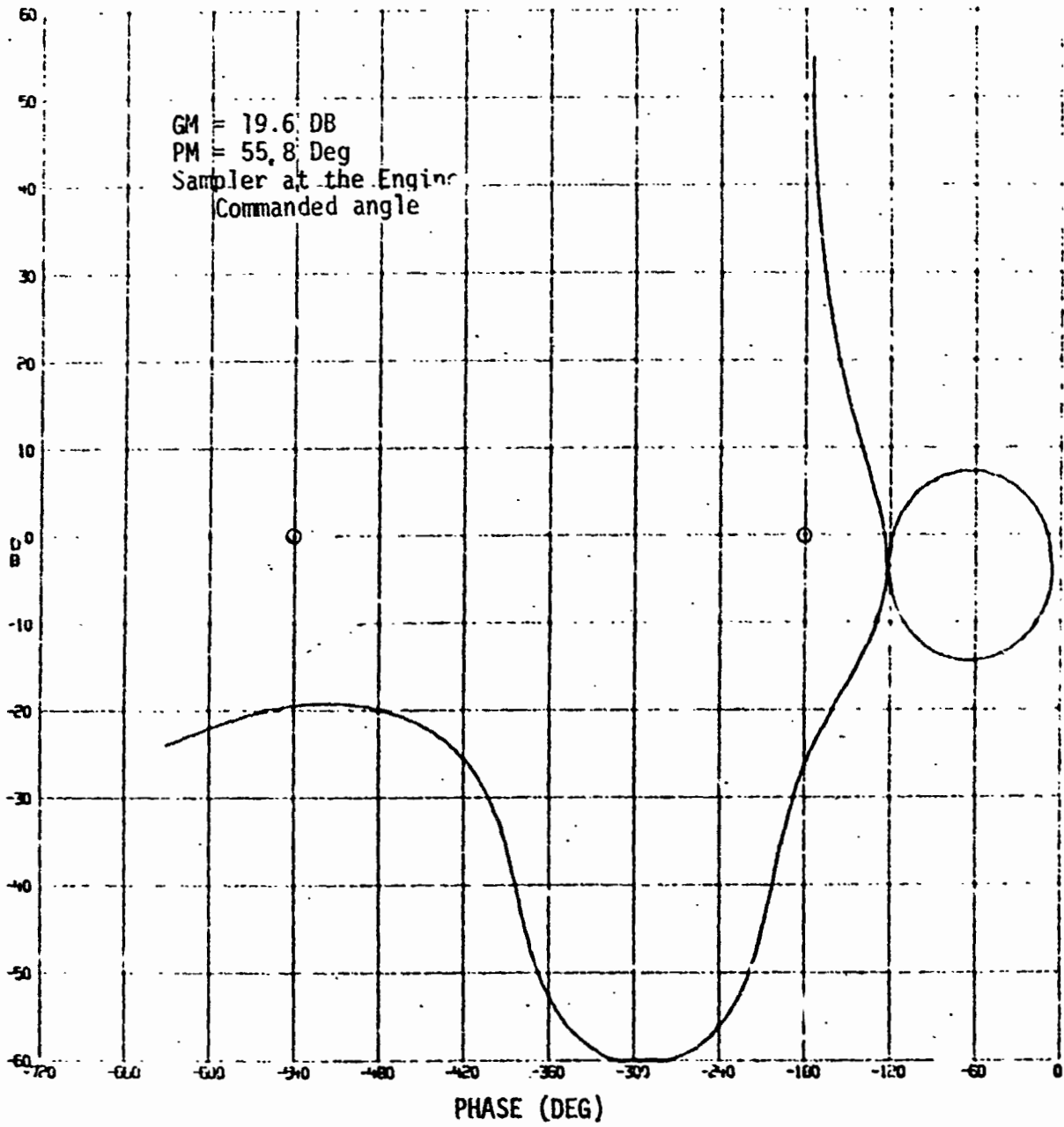


FIGURE 2. PITCH AXES NICHOLS PLOT AT IGNITION

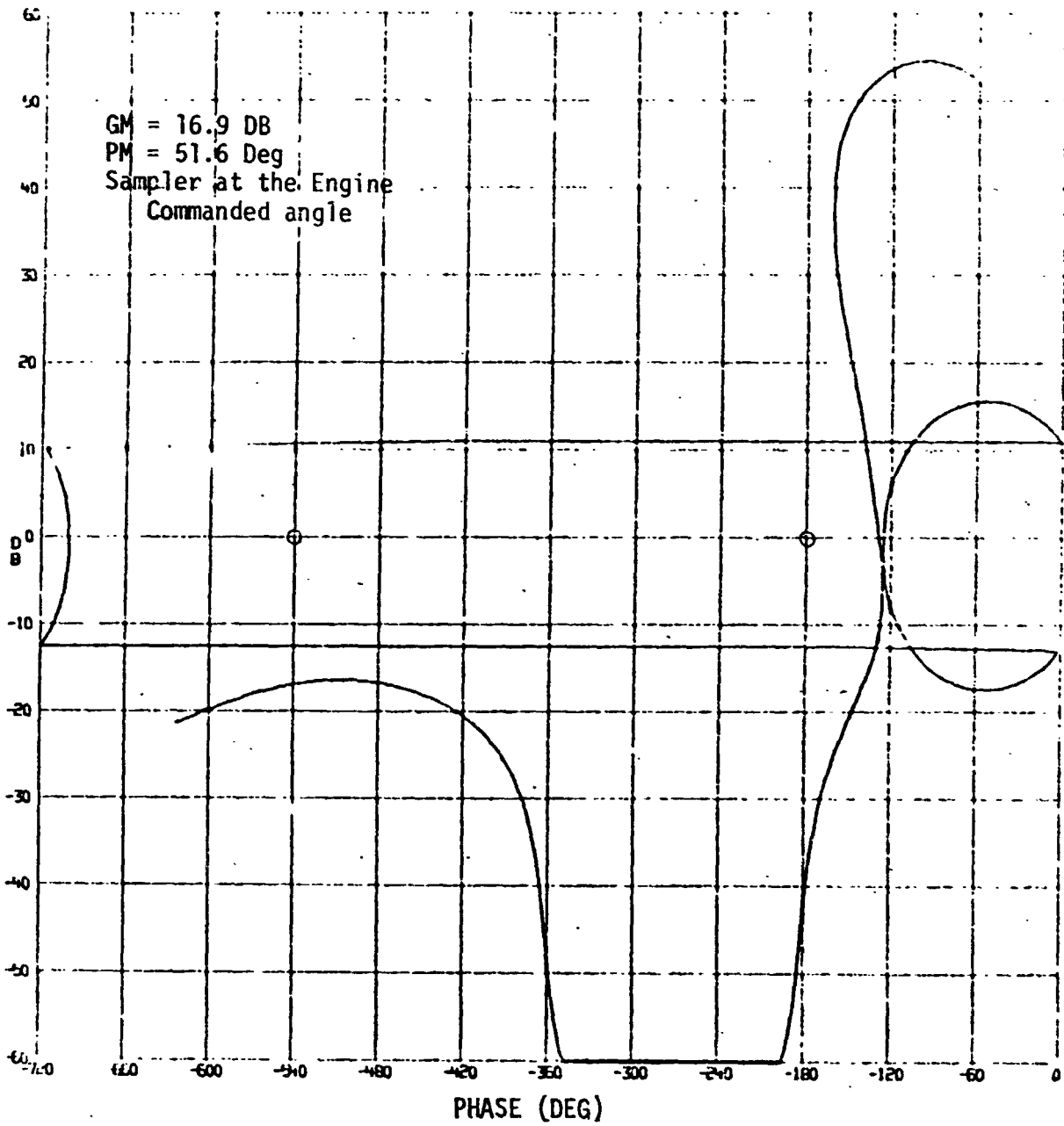


FIGURE 3. PITCH AXES NICHOLS PLOT AT 60 SECONDS

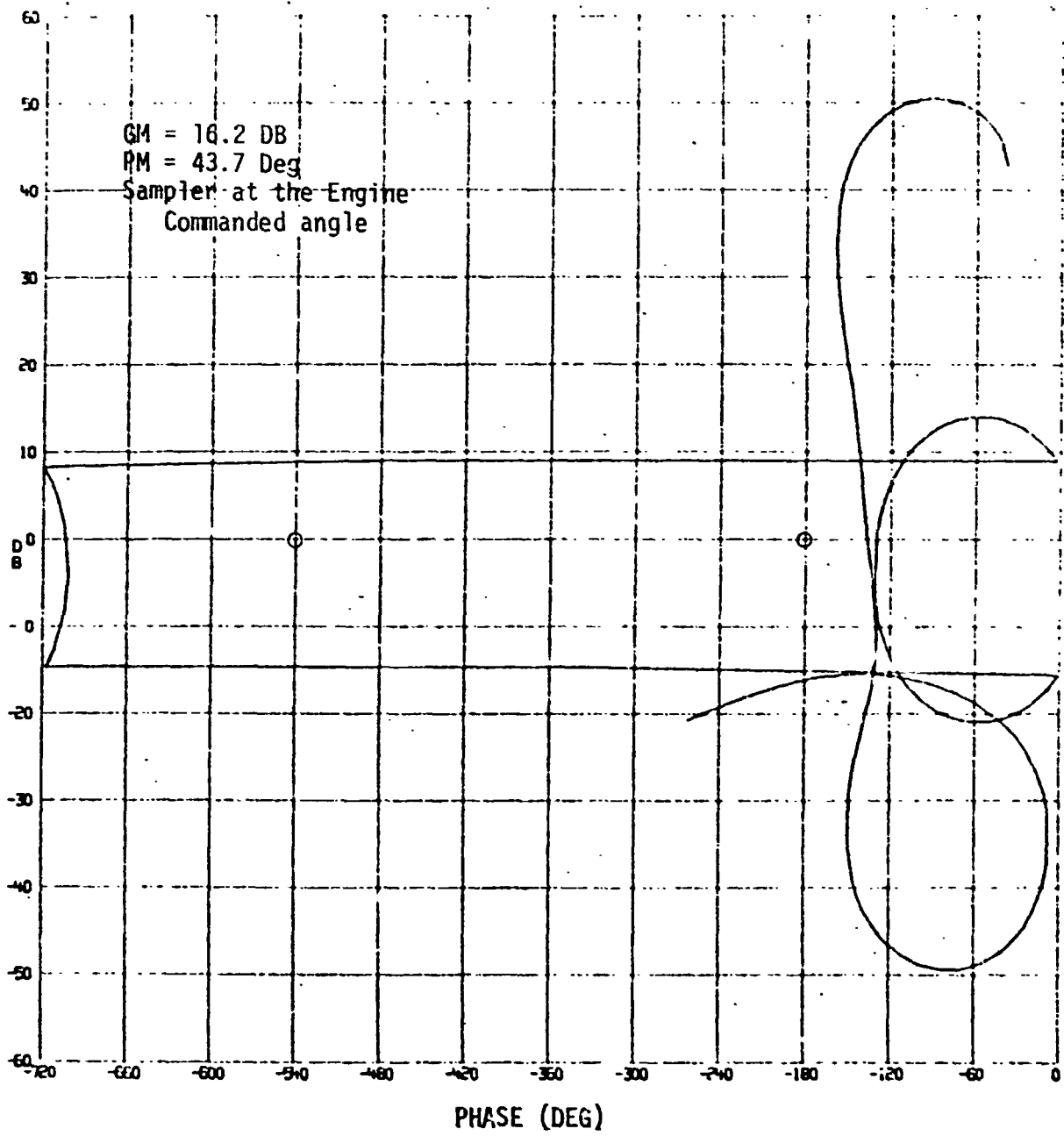


FIGURE 4. PITCH AXES NICHOLS PLOT AT MAX Q

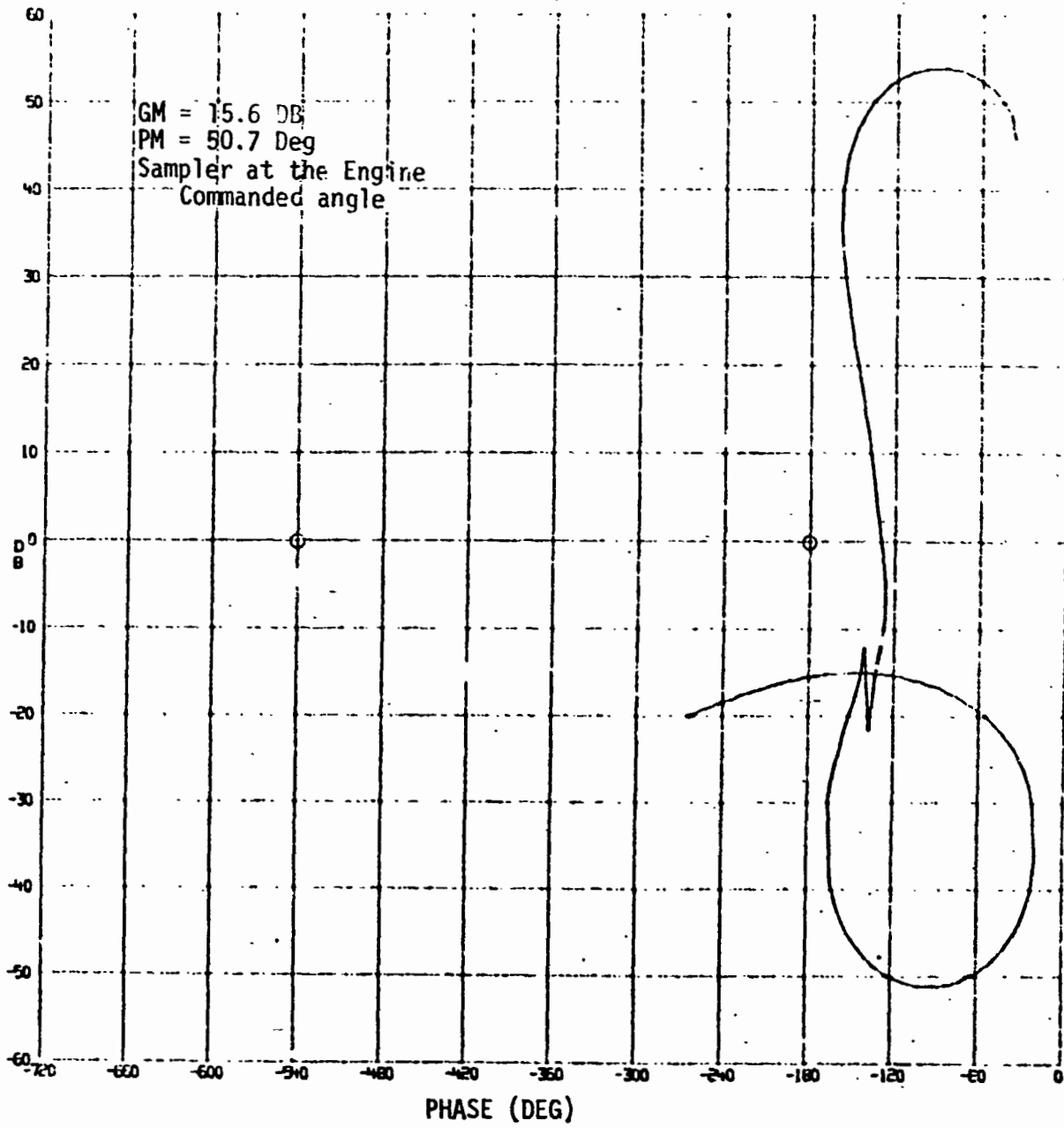


FIGURE 5. PITCH AXES NICHOLS PLOT AT 70 SECONDS

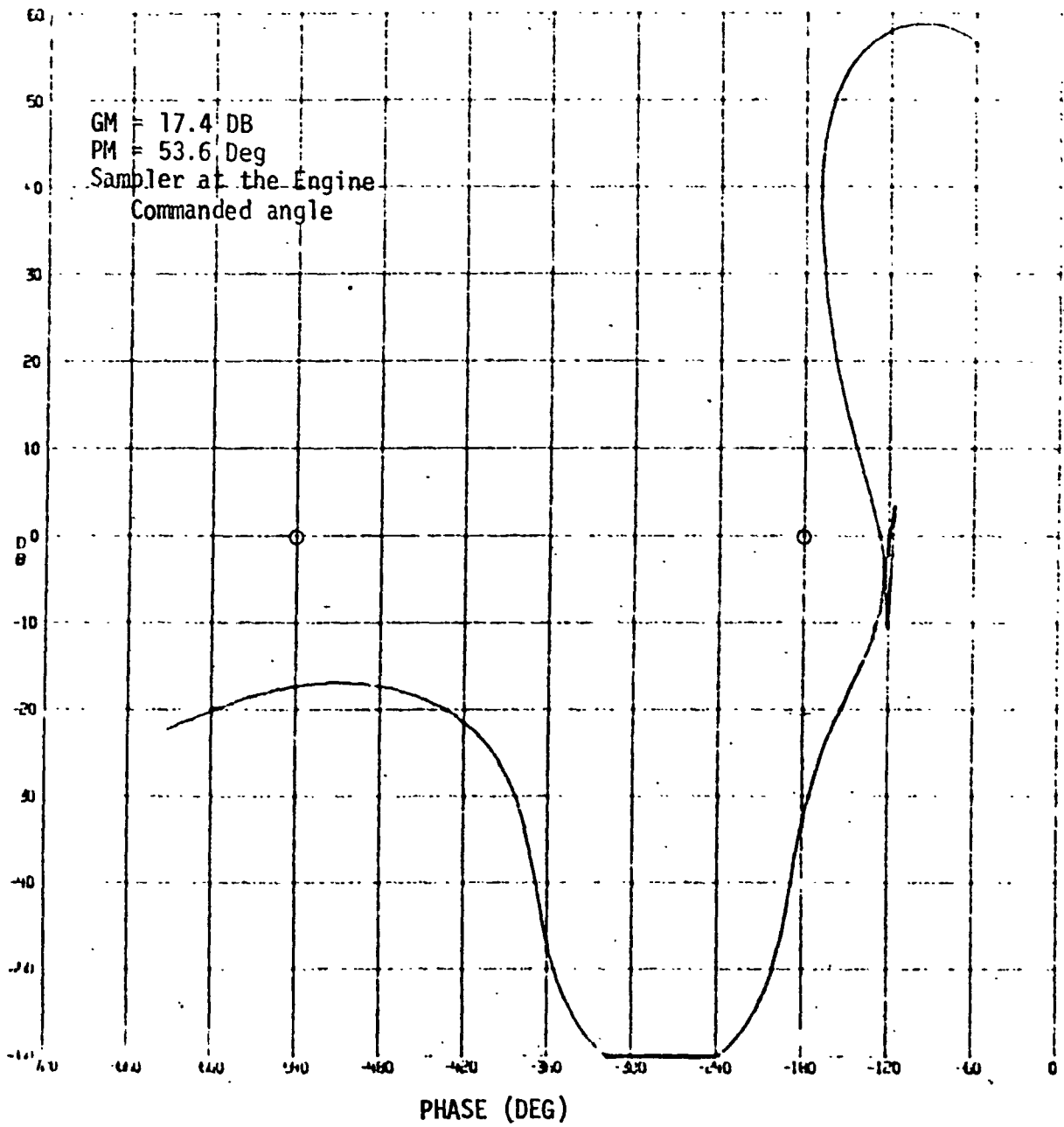


FIGURE 6. PITCH AXES NICHOLS PLOT AT 95 SECONDS

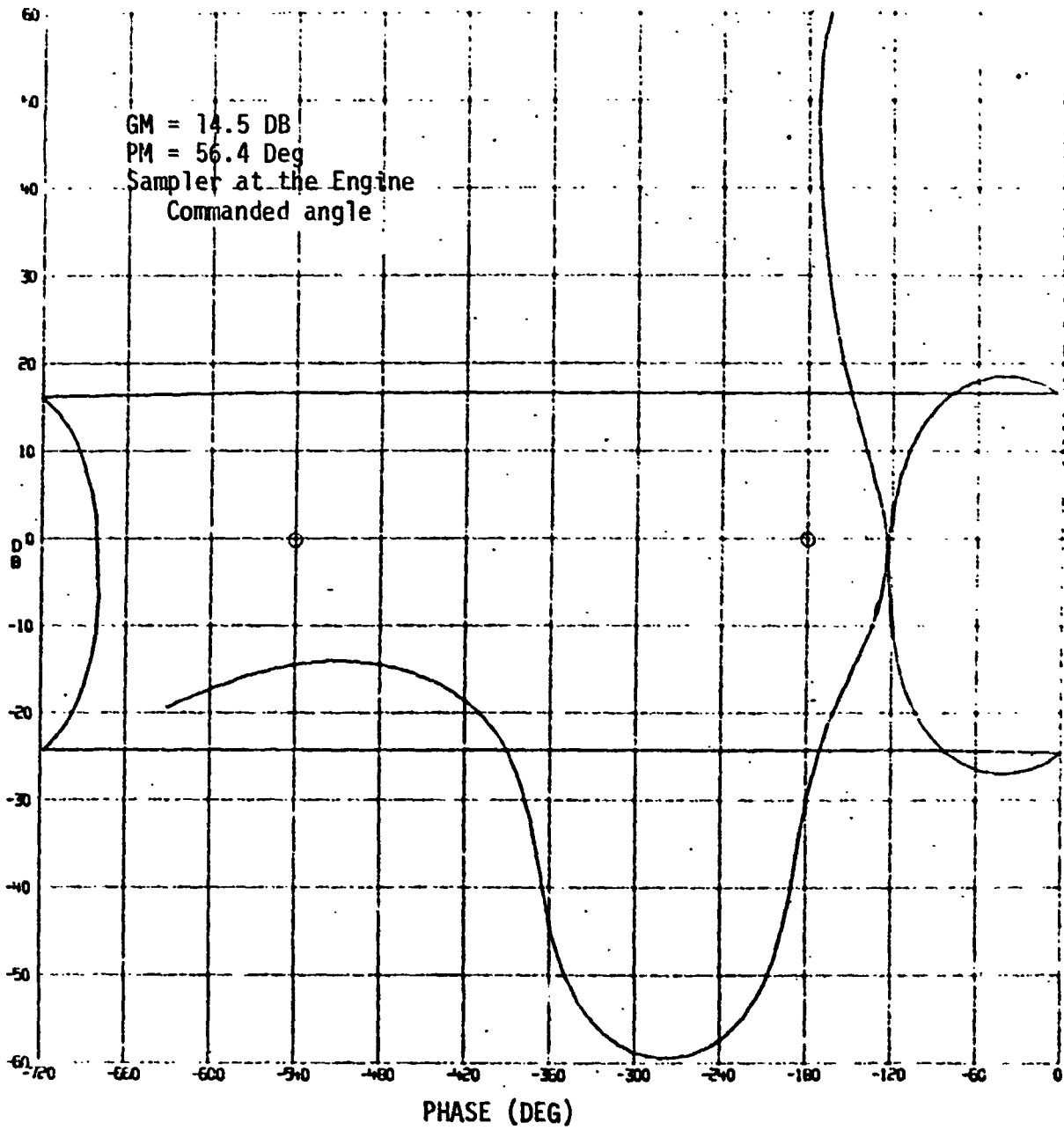


FIGURE 7. PITCH AXES NICHOLS PLOT AT 115 SECONDS

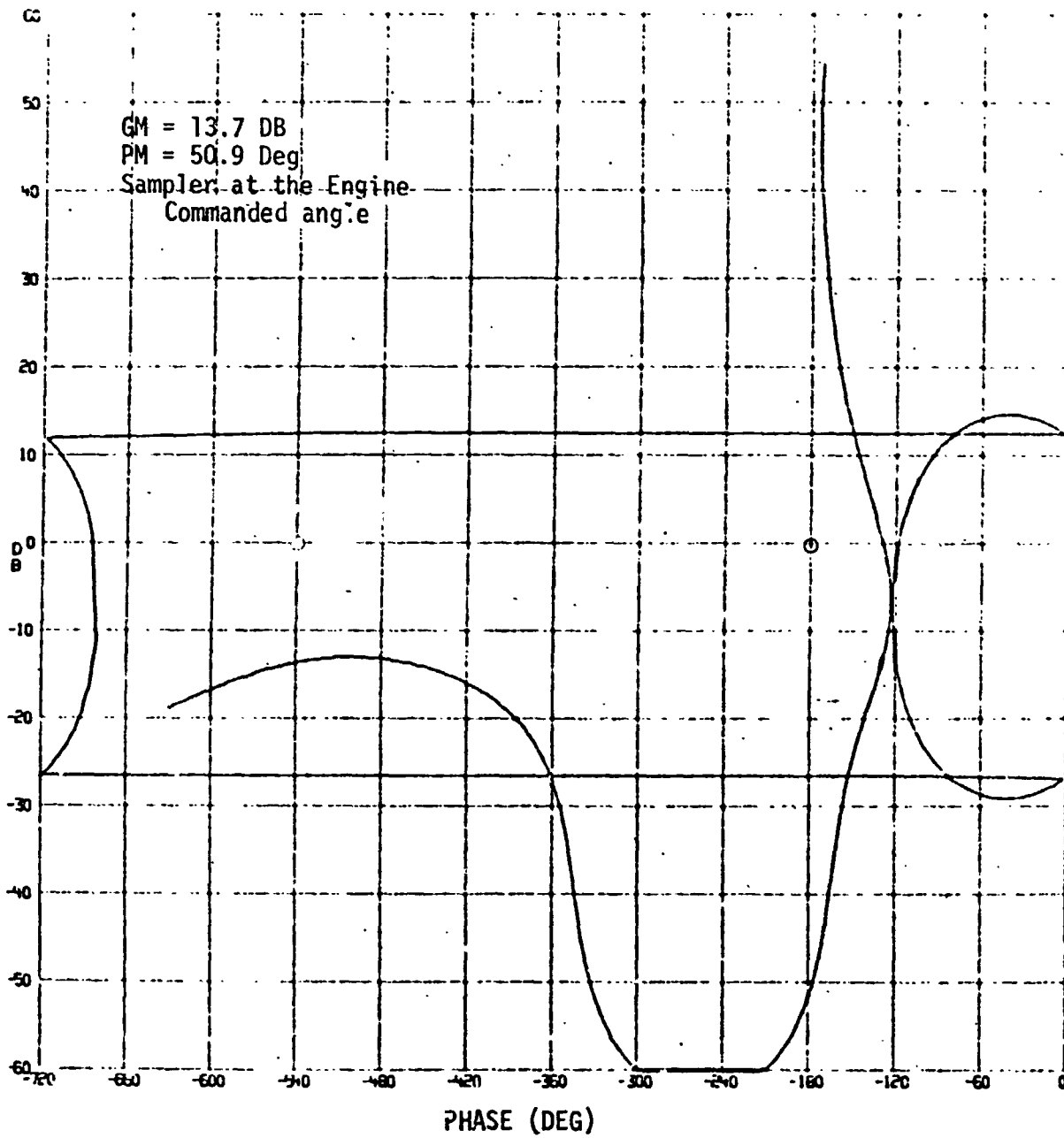


FIGURE 8. PITCH AXES NICHOLS PLOT AT 120 SECONDS

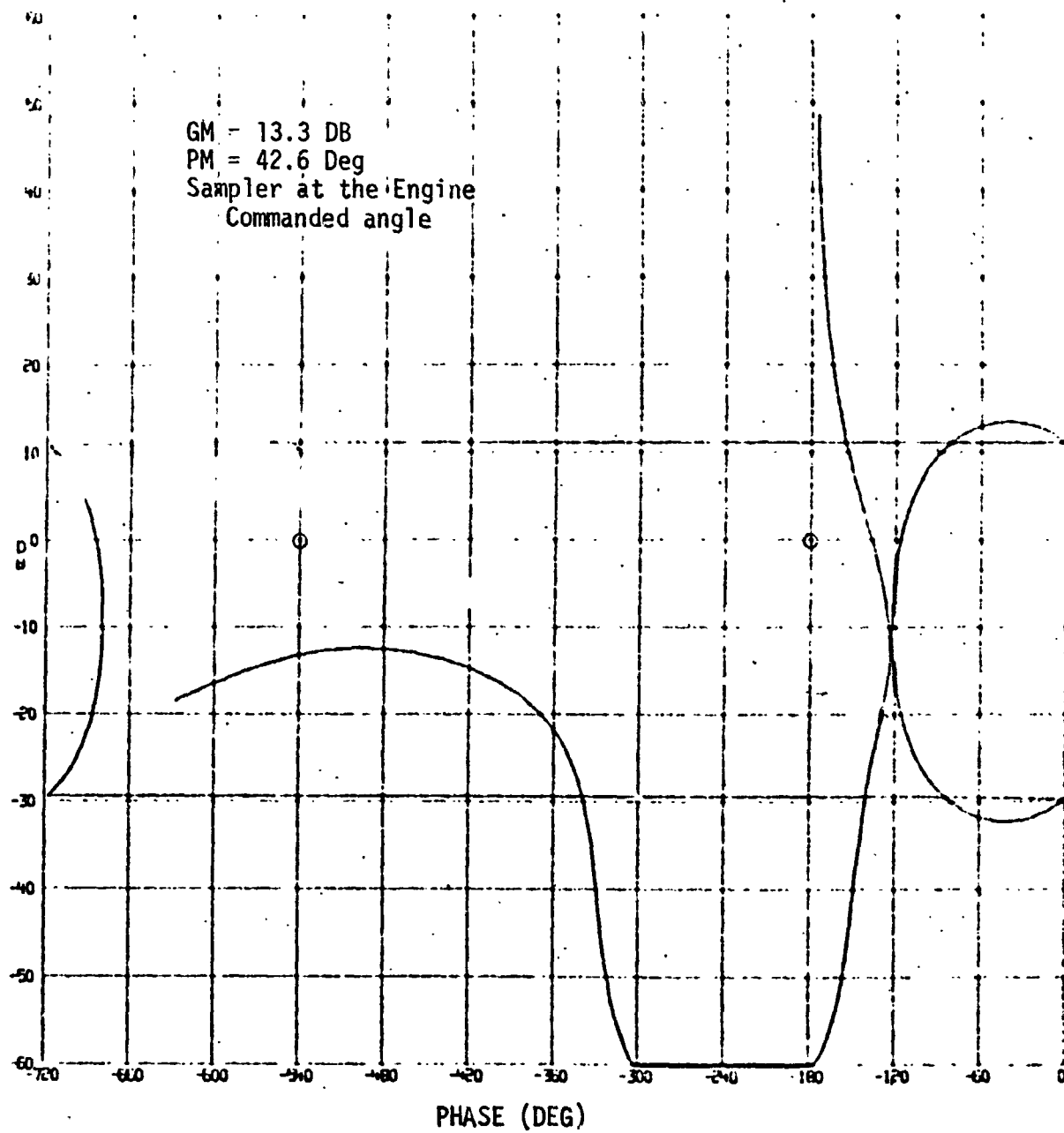


FIGURE 9. PITCH AXES NICHOLS PLOT AT SRM BURNOUT

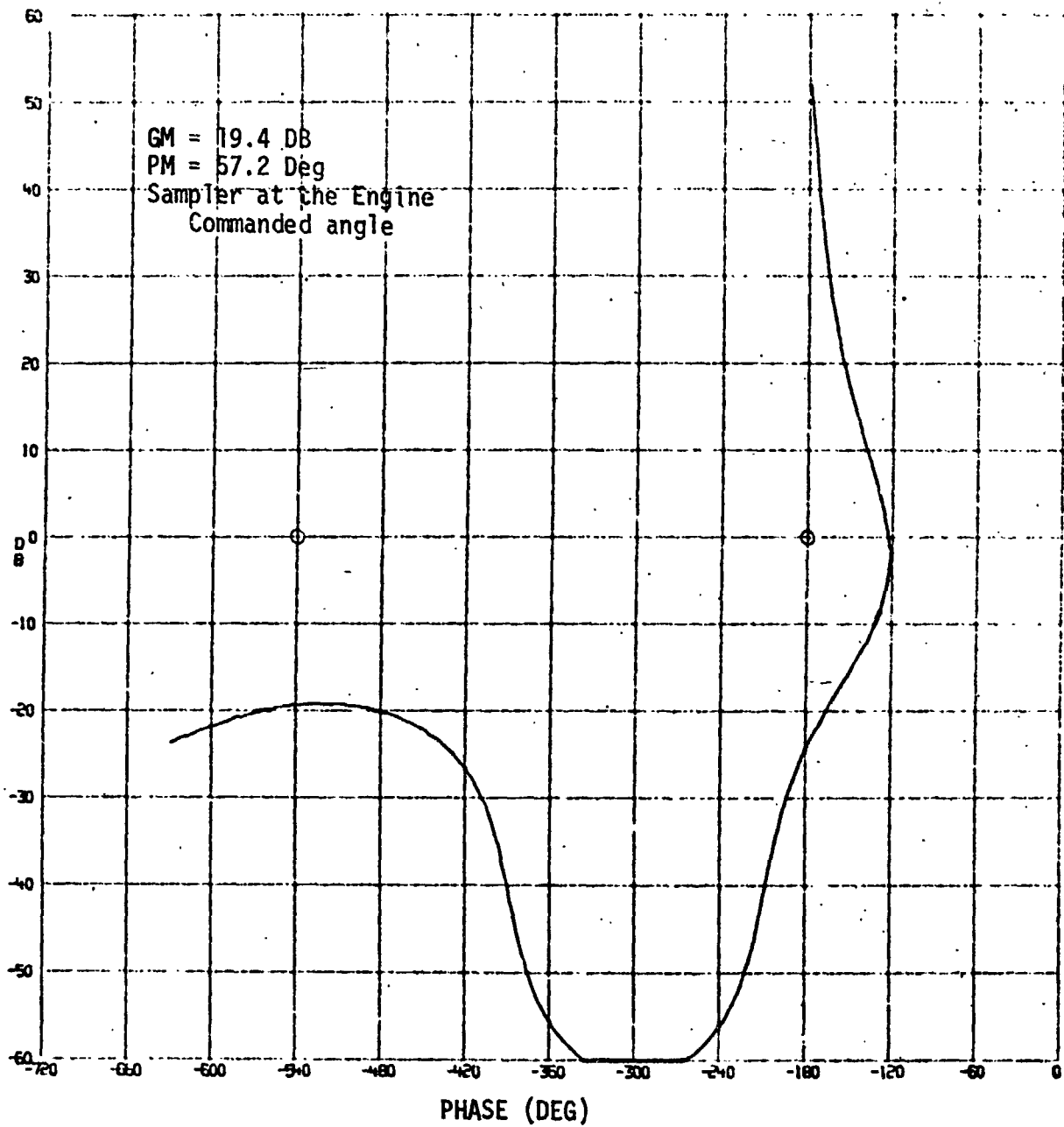


FIGURE 10. YAW AXES NICHOLS PLOT AT IGNITION

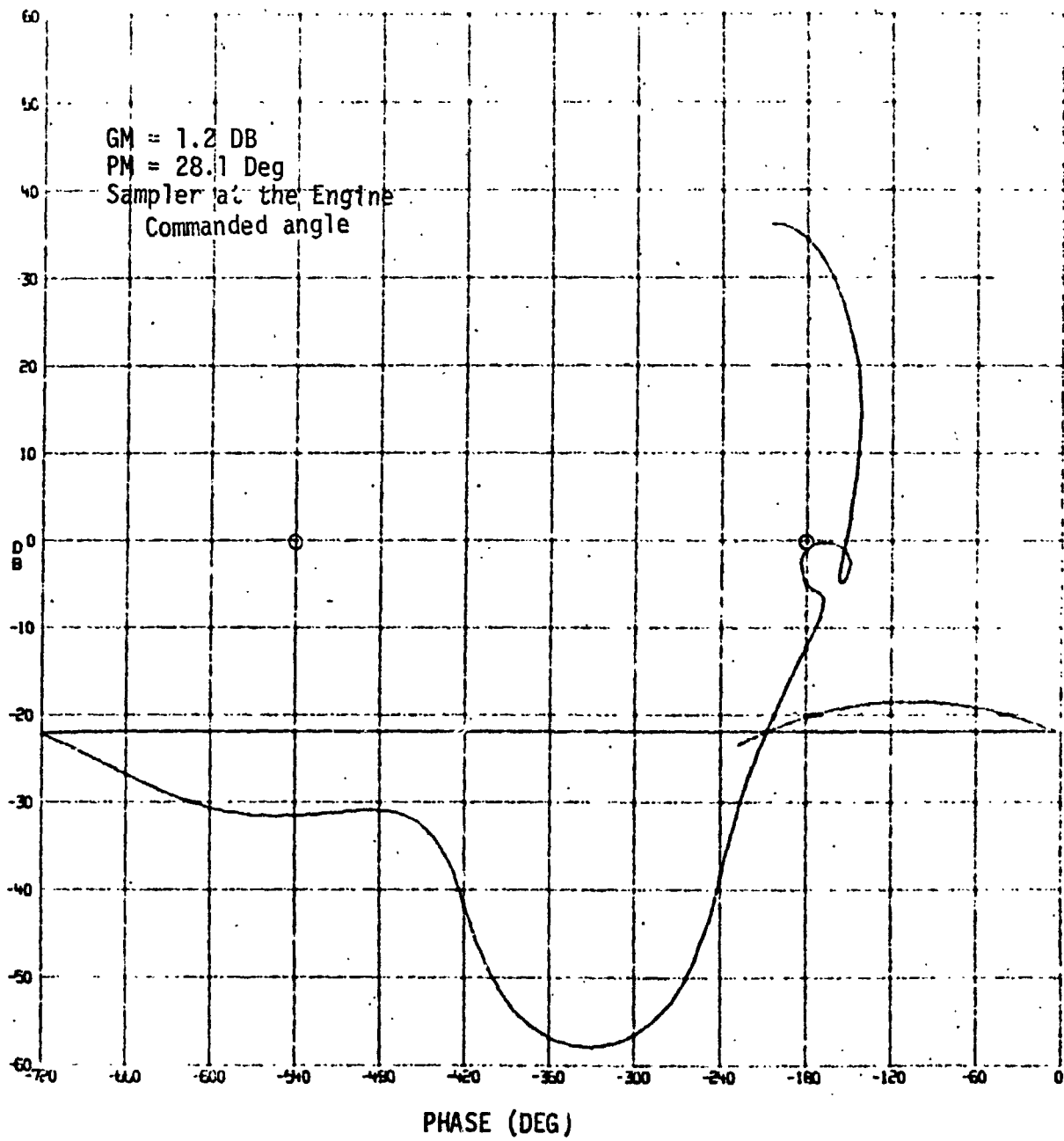


FIGURE 11. YAW AXES NICHOLS PLOT AT 60 SECONDS

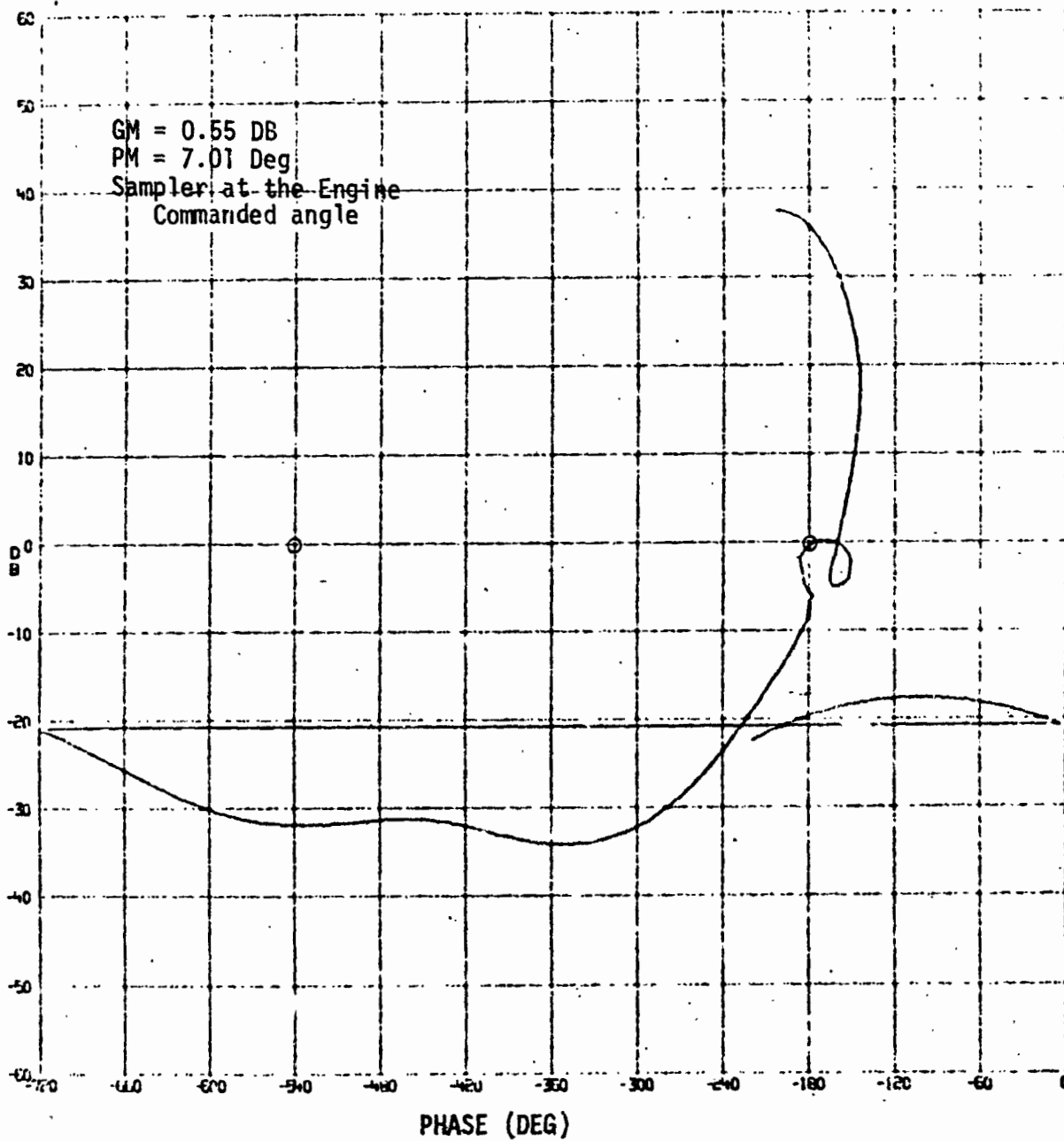


FIGURE 12. YAW AXES NICHOLS PLOT AT MAX Q

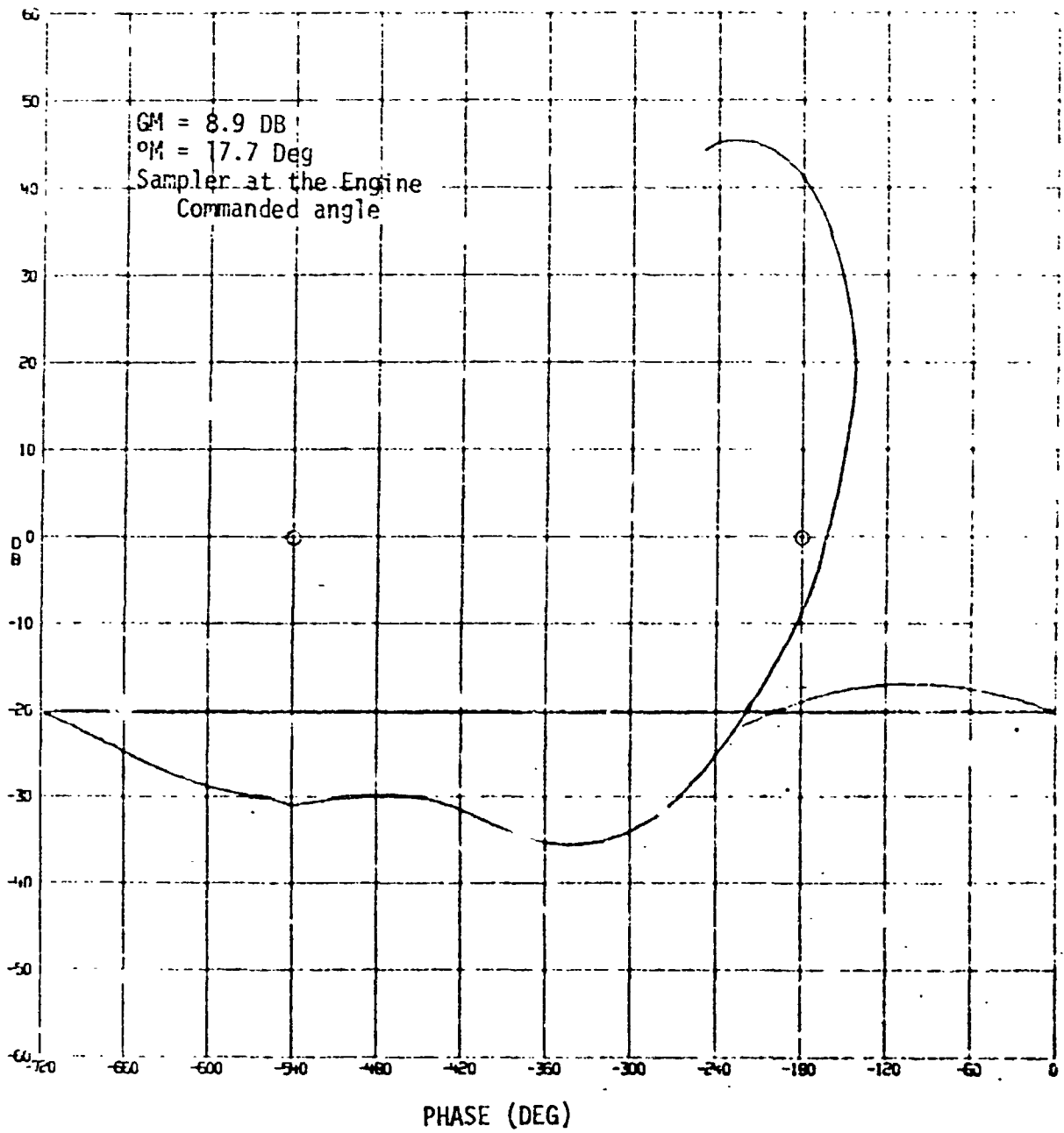


FIGURE 13. YAW AXES NICHOLS PLOT AT 70 SECONDS

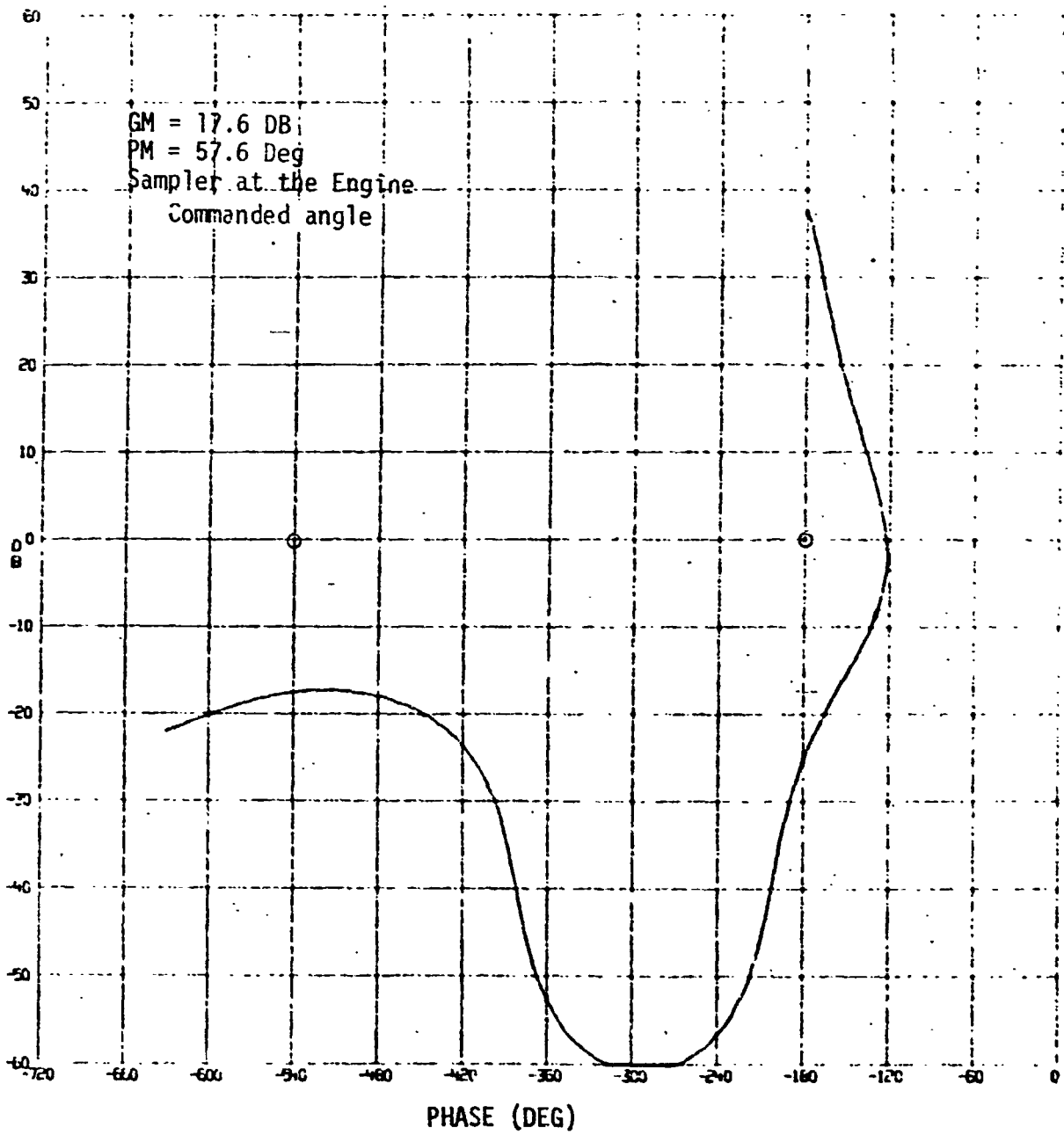


FIGURE 14. YAW AXES NICHOLS PLOT AT 95 SECONDS

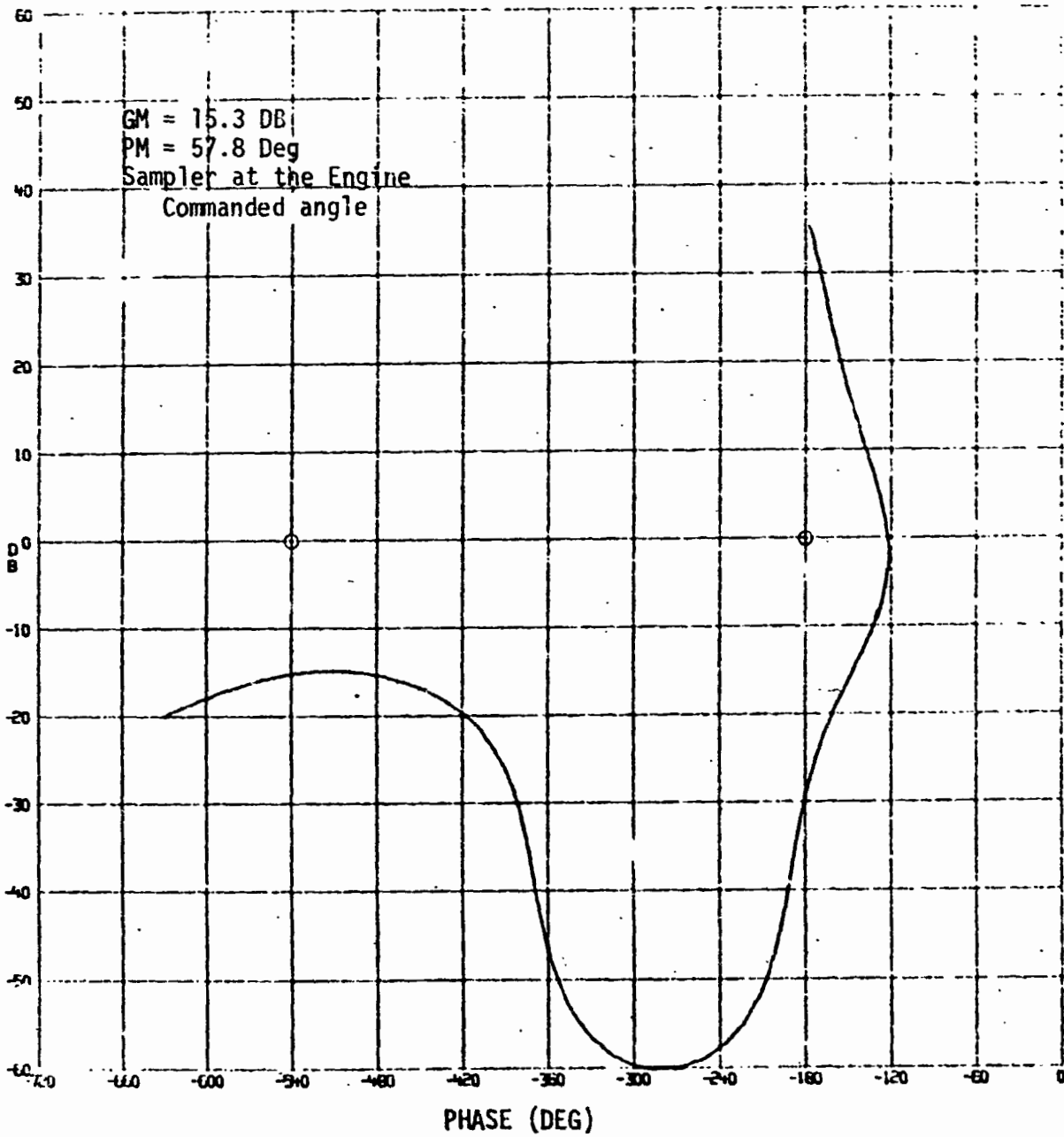


FIGURE 15. YAW AXES NICHOLS PLOT AT 115 SECONDS

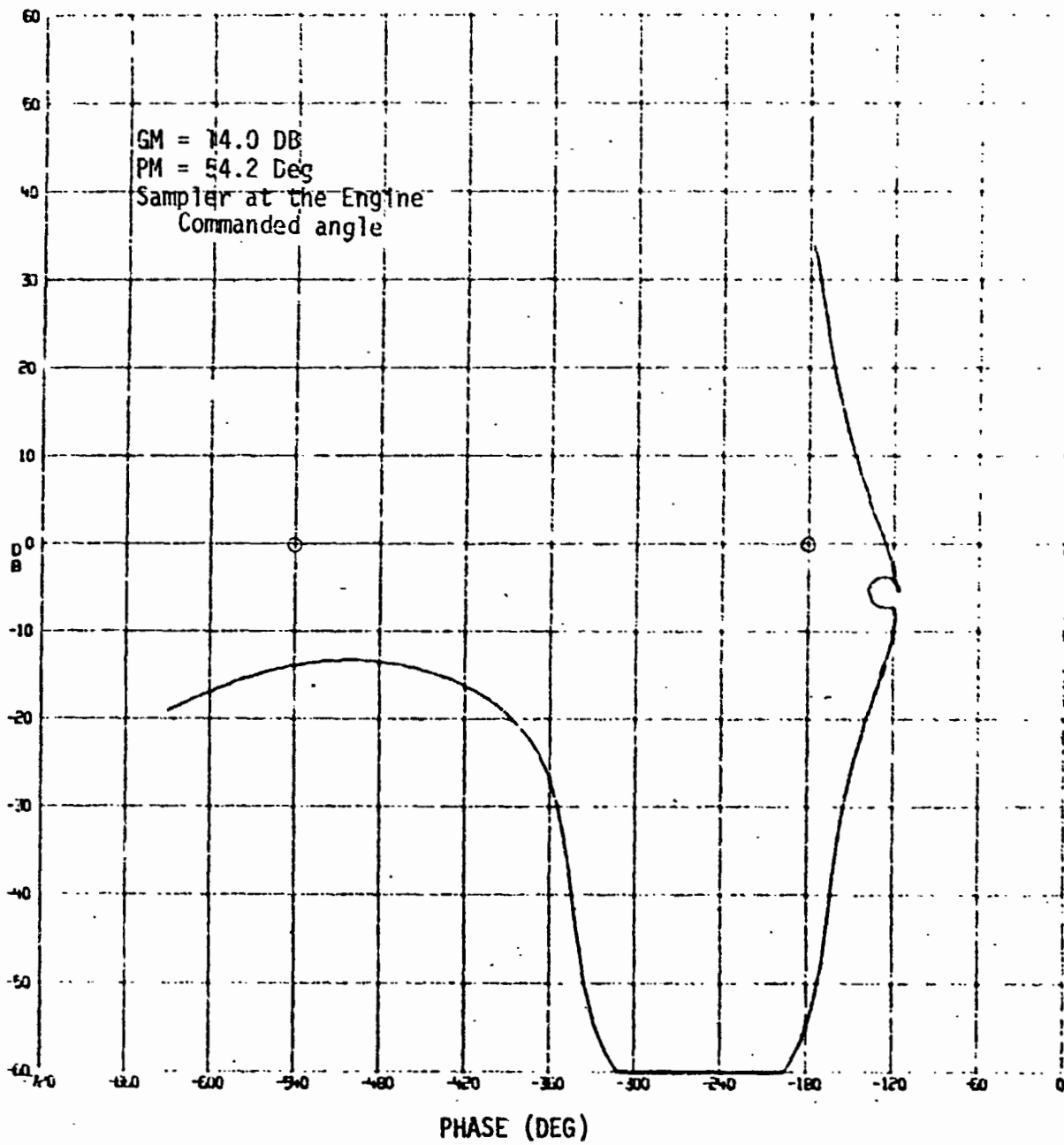


FIGURE 16. YAW AXES NICHOLS PLOT AT 120 SECONDS

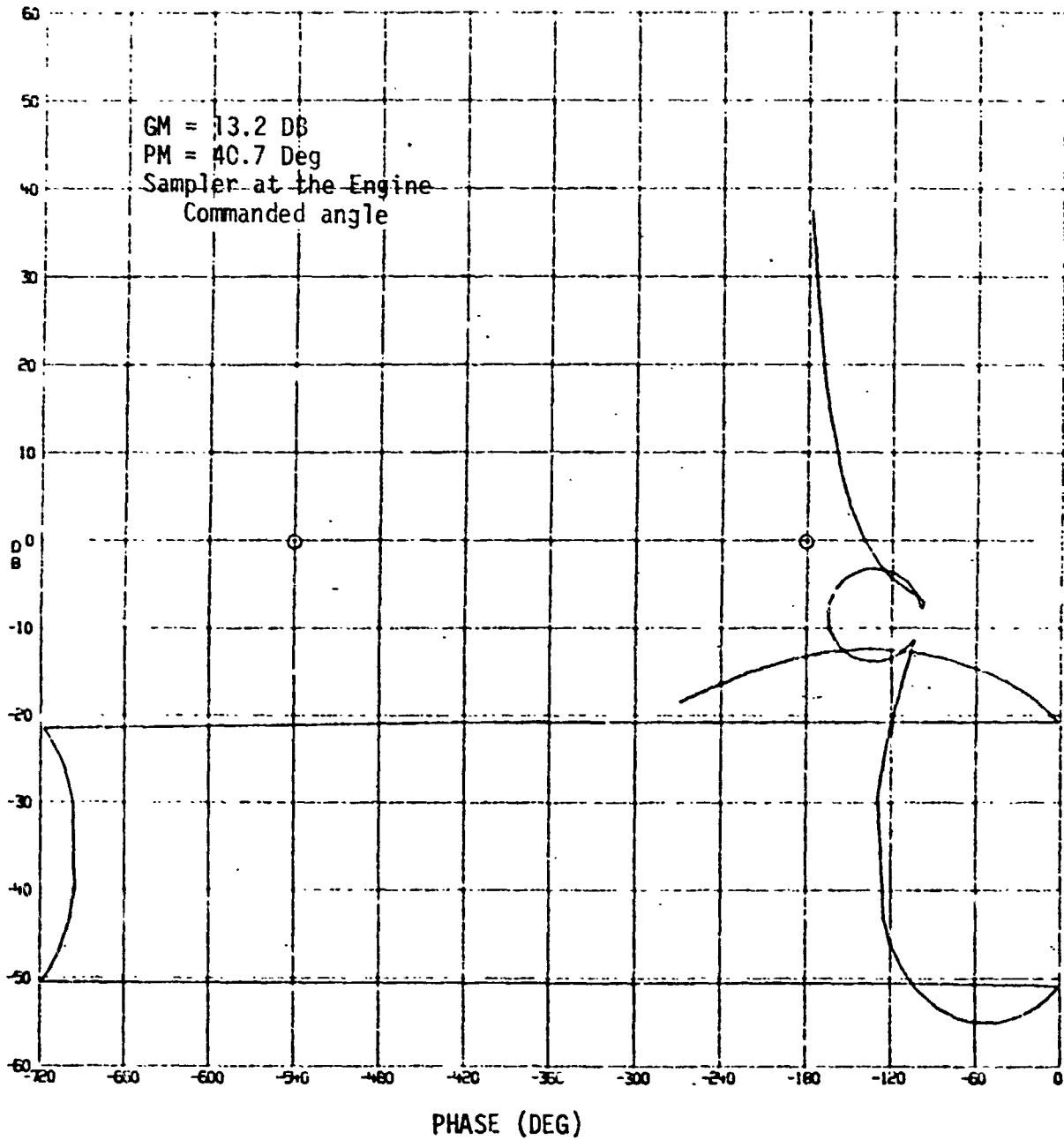


FIGURE 17. YAW AXES NICHOLS PLOT AT SRM BURNOUT

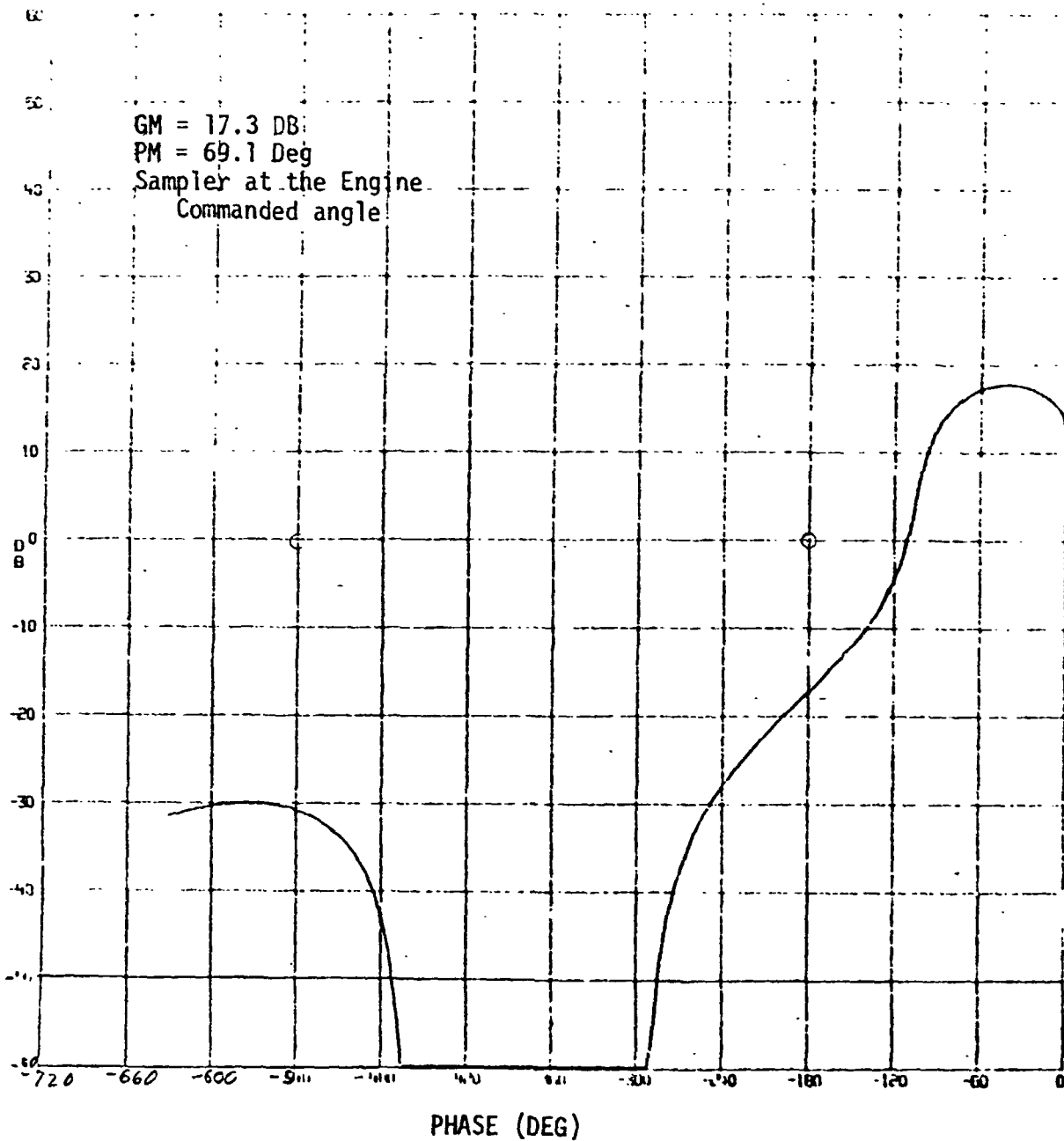


FIGURE 18. ROLL AXES NICHOLS PLOT AT IGNITION

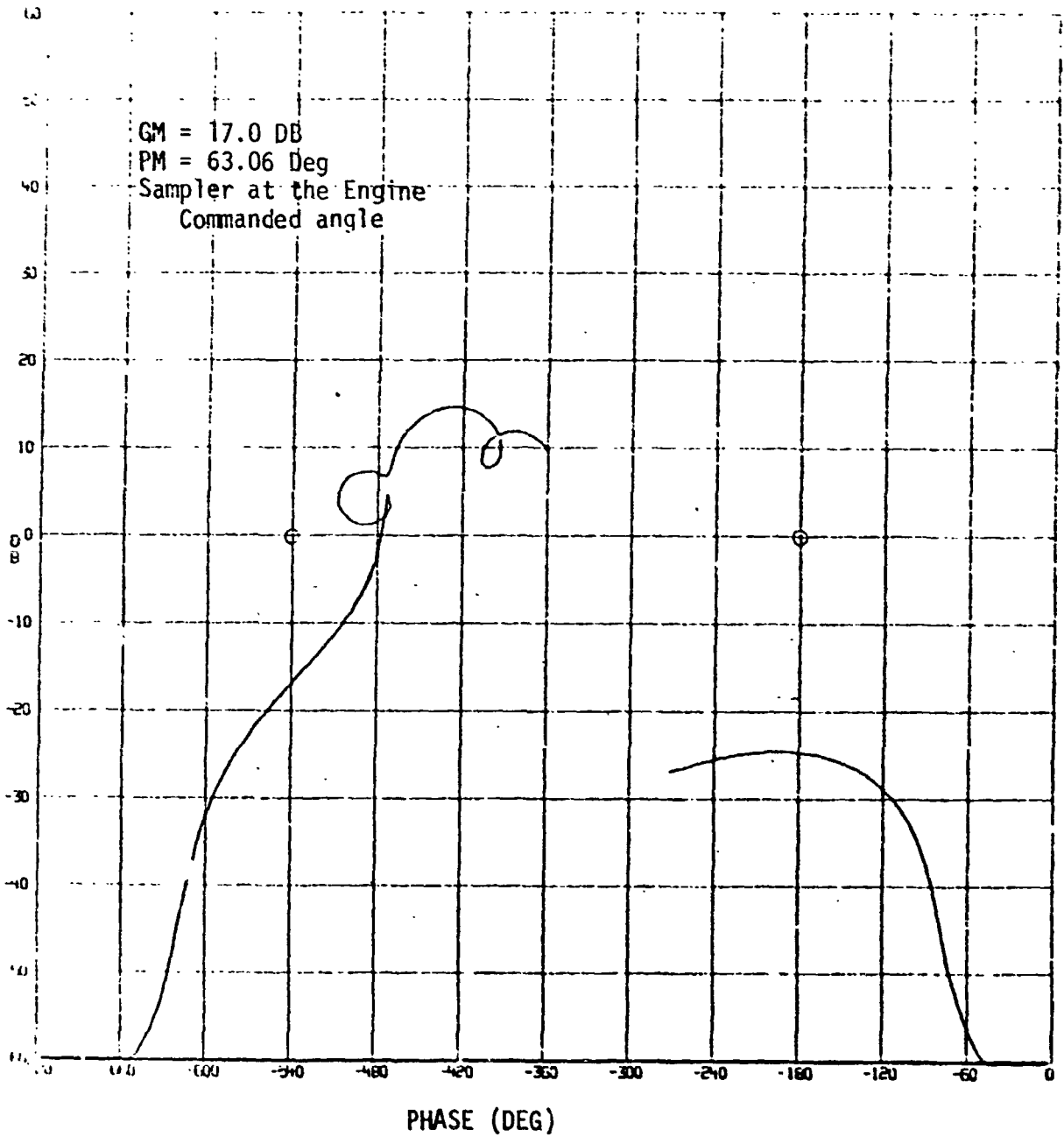


FIGURE 19. ROLL AXES NICHOLS PLOT AT 60 SECONDS

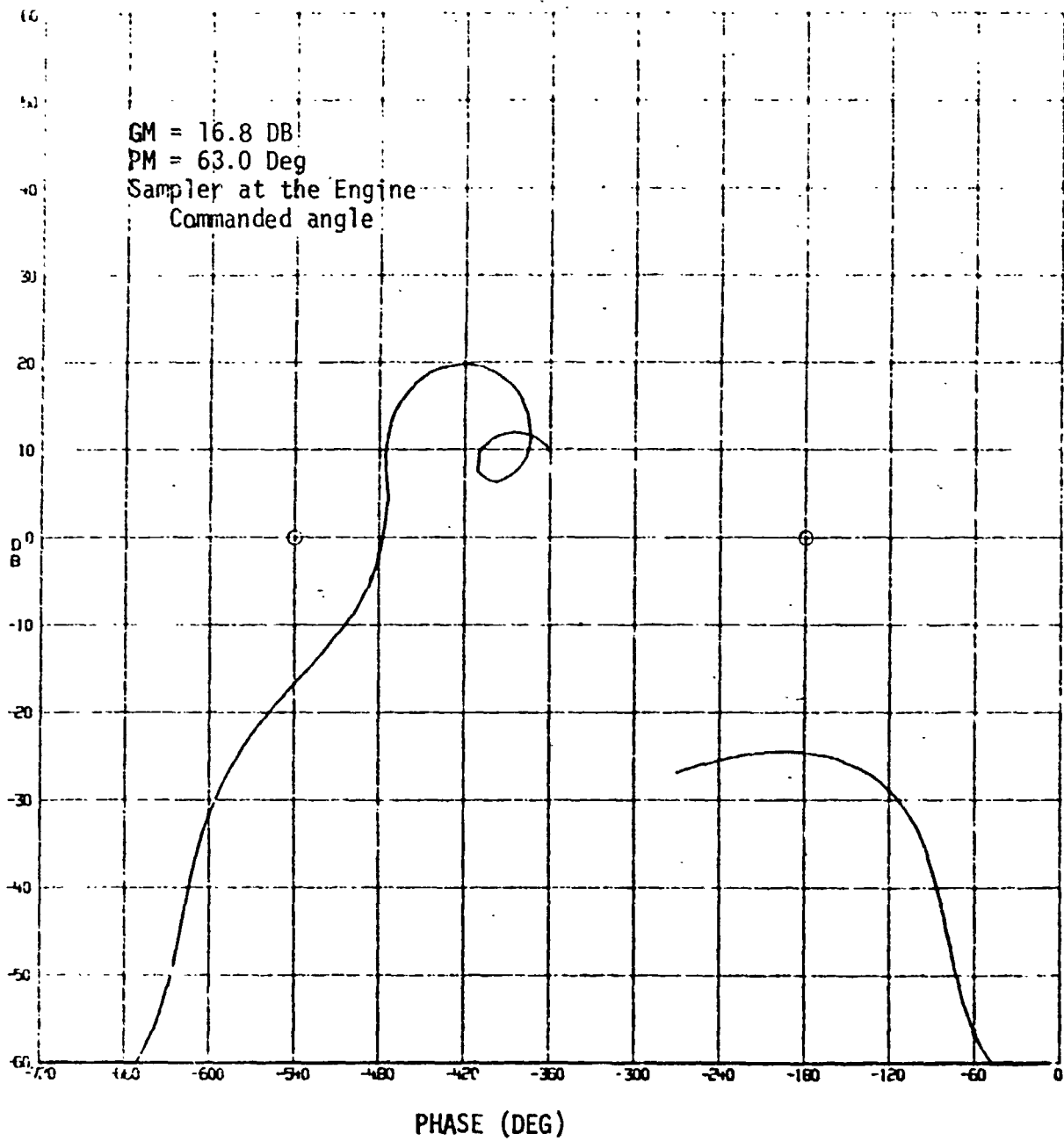


FIGURE 20. ROLL AXES NICHOLS PLOT AT MAX Q

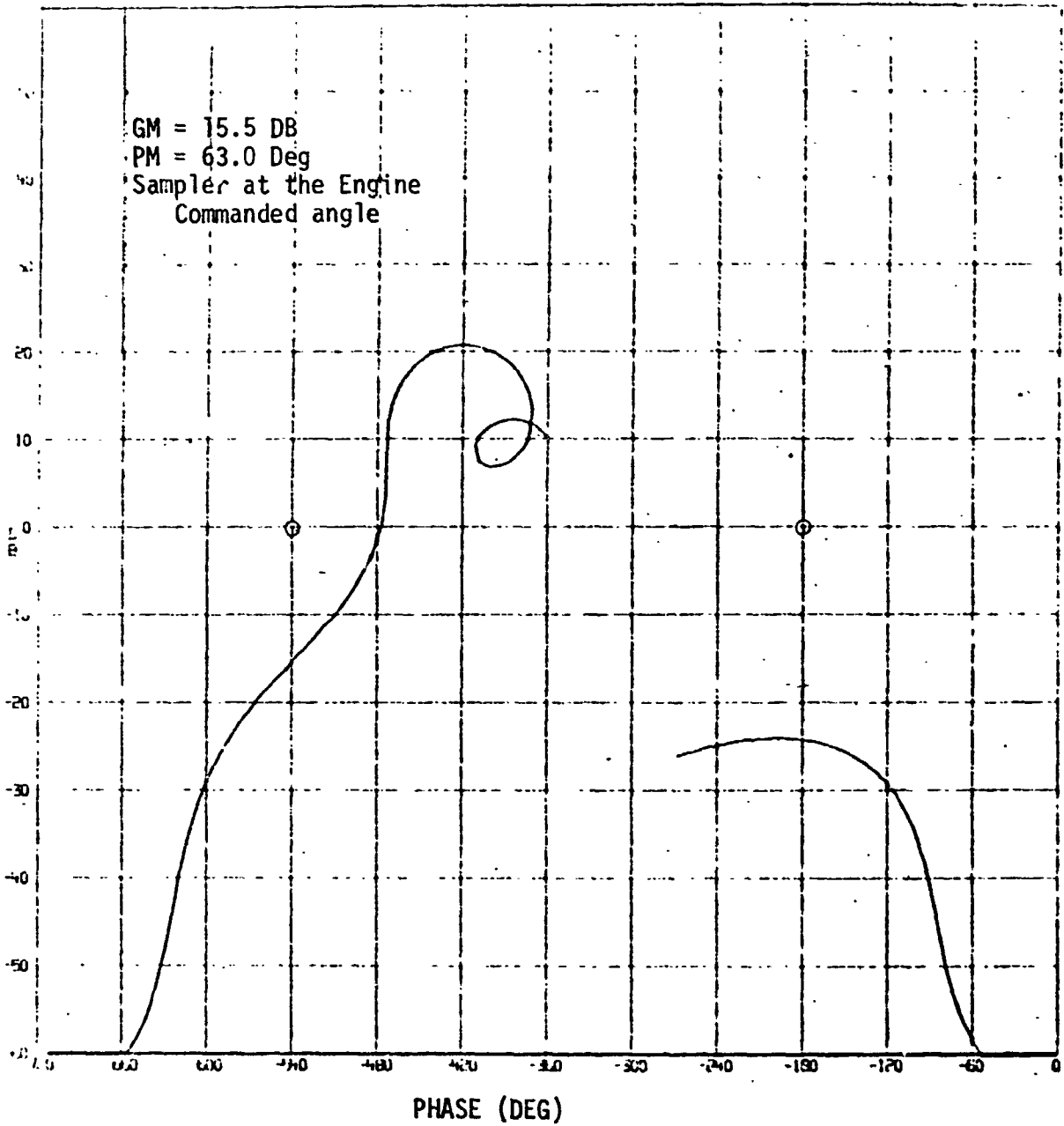


FIGURE 21. ROLL AXES NICHOLS PLOT AT 70 SECONDS

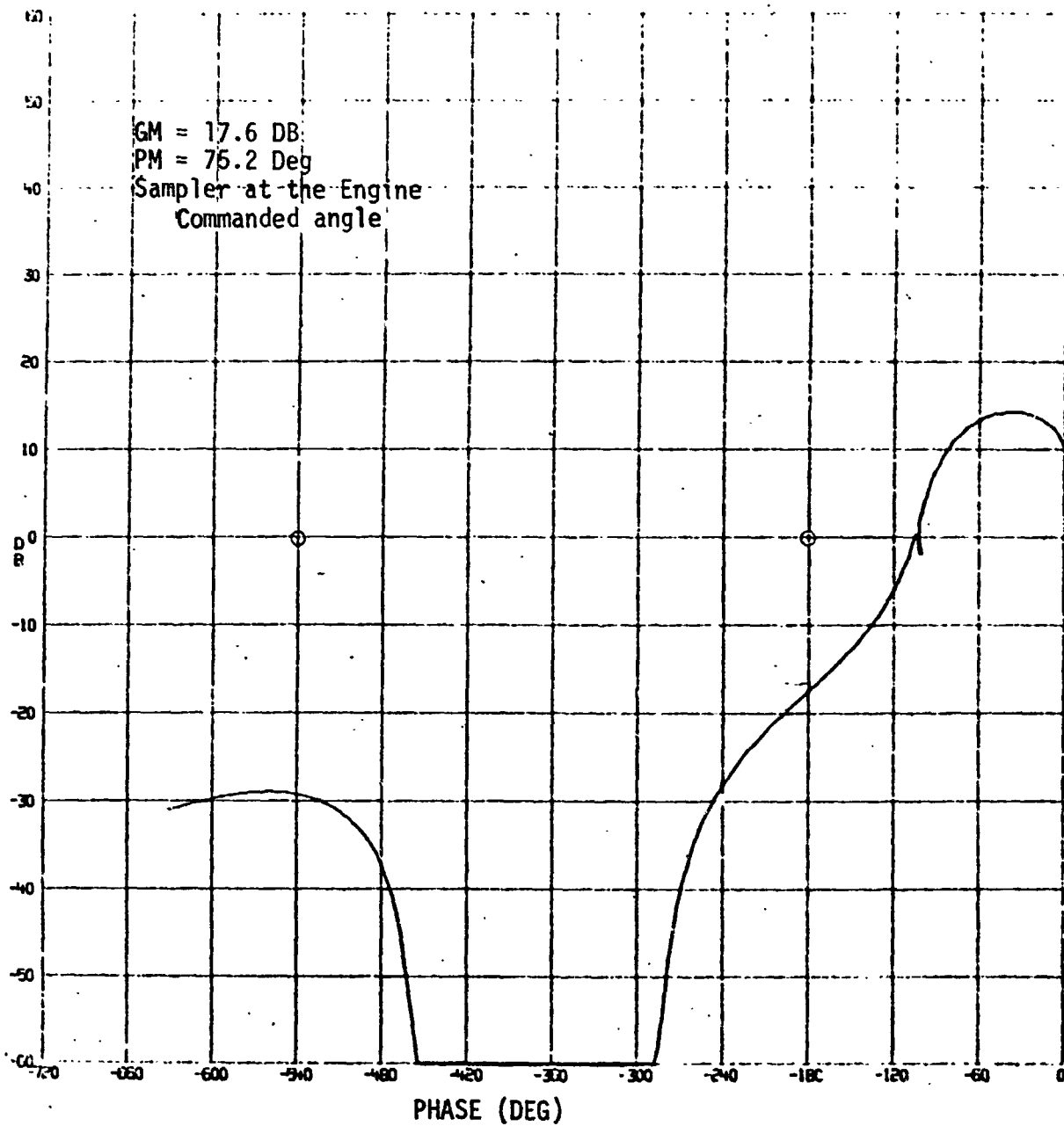


FIGURE 22. ROLL AXES NICHOLS PLOT AT 95 SECONDS

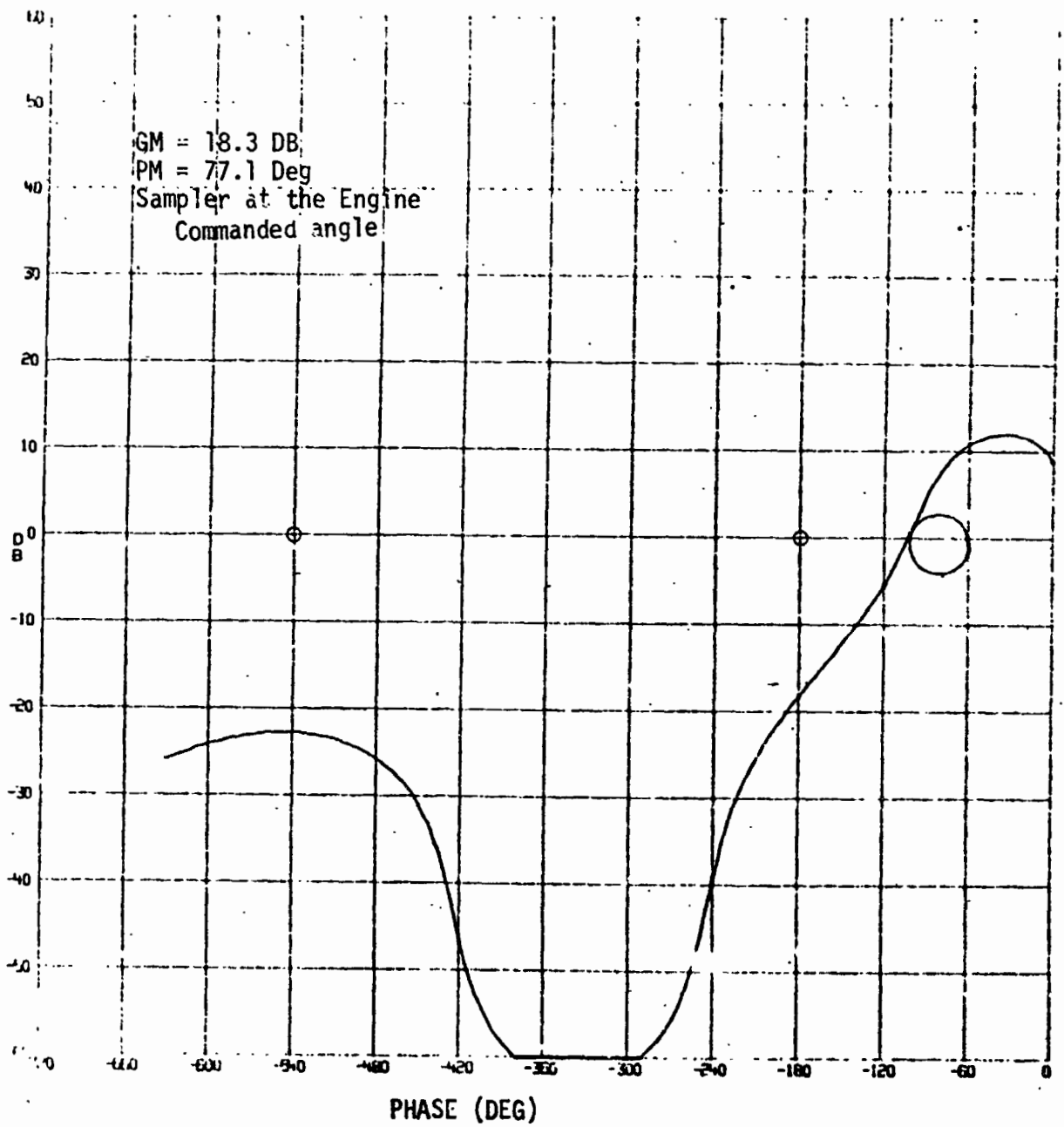


FIGURE 23. ROLL AXES NICHOLS PLOT AT 115 SECONDS

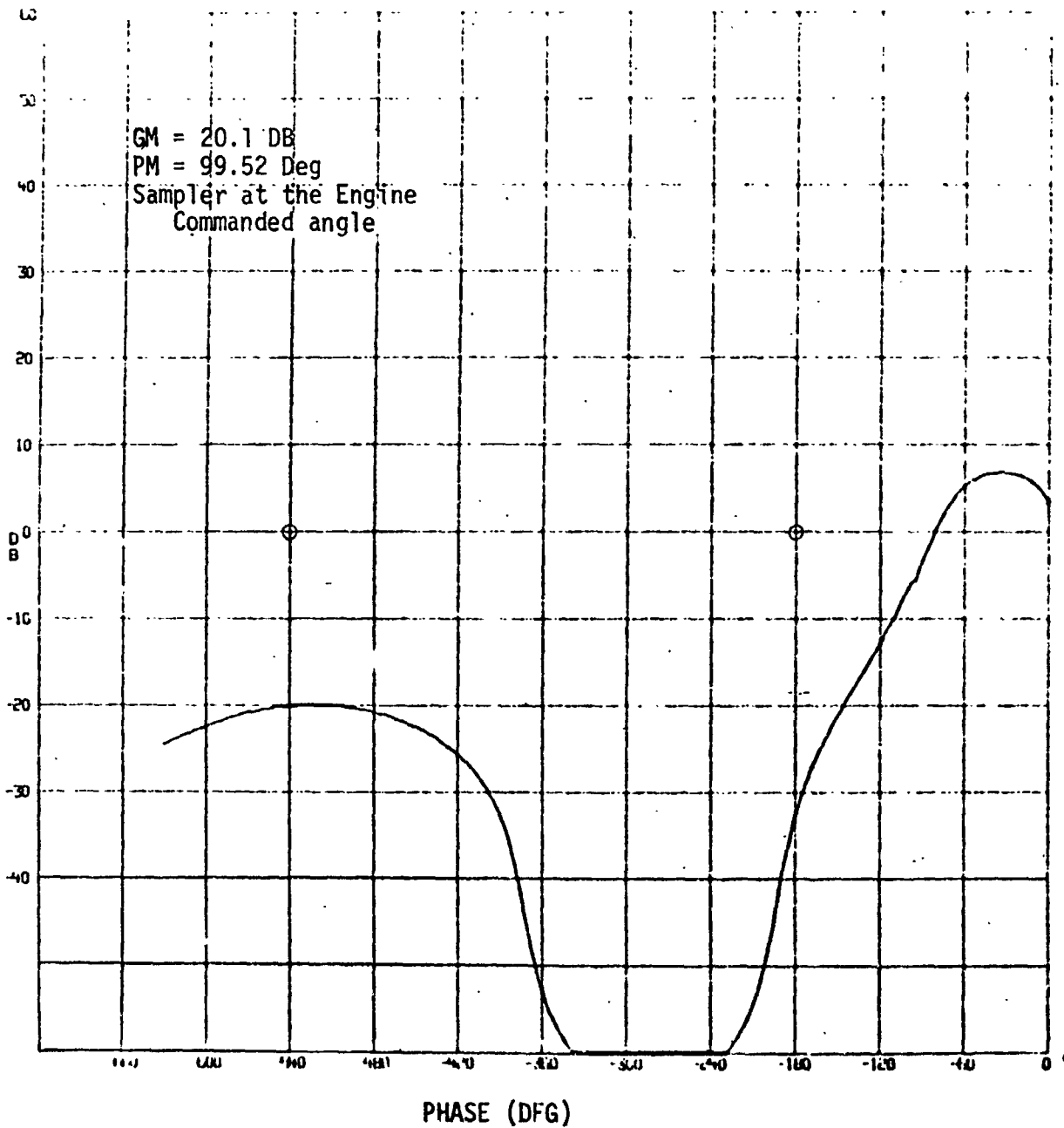


FIGURE 24. ROLL AXES NICHOLS PLOT AT 120 SECONDS

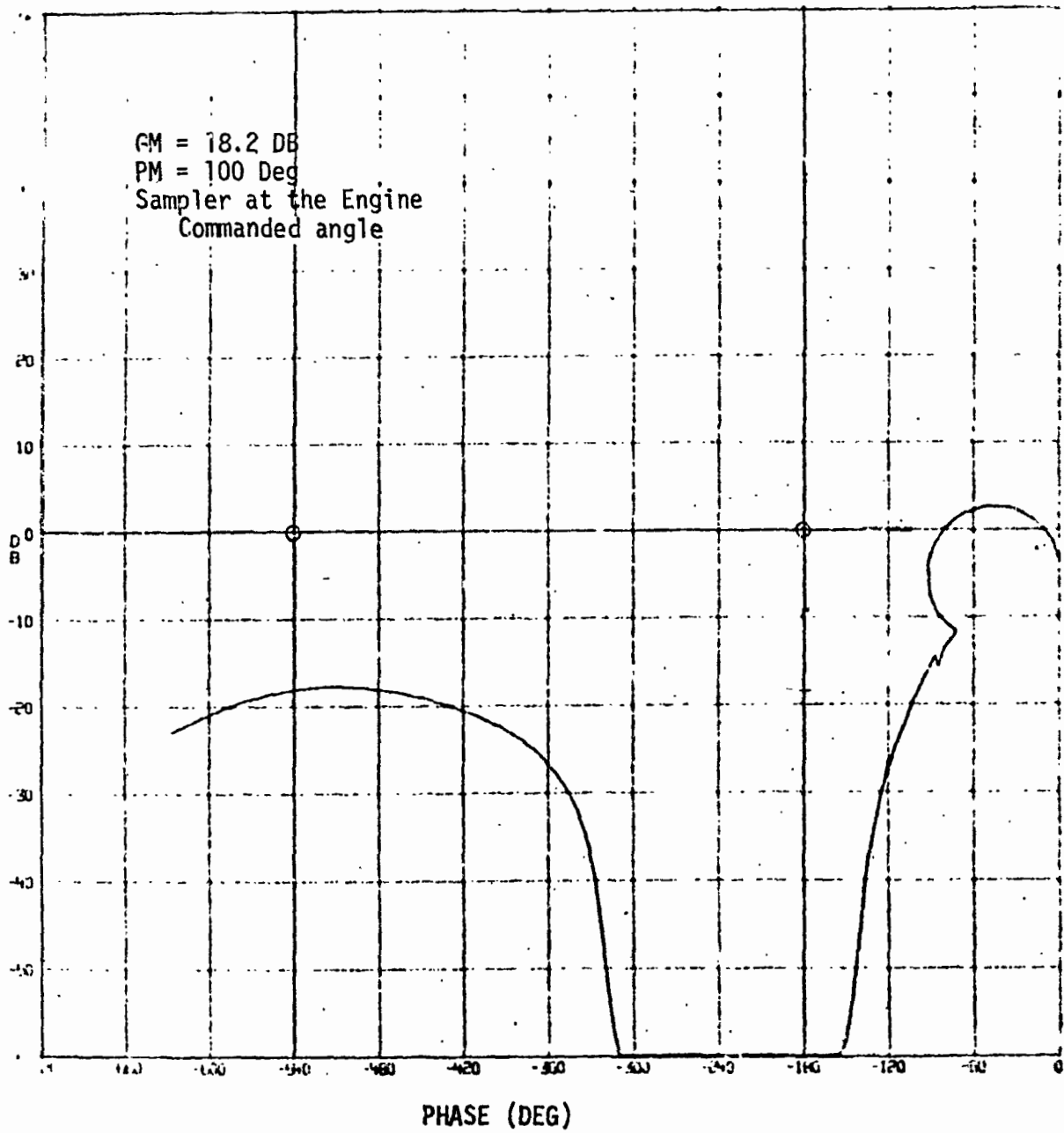


FIGURE 25. ROLL AXES NICHOLS PLOT AT SRM BURNOUT

3.6 BENDING STABILITY

Pitch axes stability margins with rigid body and one slosh mode were determined (see Section 3.5.1). The max Q time point was selected to perform an evaluation of the effect of bending on vehicle stability. Bending data was obtained and is listed in Table I.

Preliminary filters were selected and described in Table II. Optimization of the filters was not attempted. The filters were taken from the following reference:

NASA Memorandum EV3-74-25, "Minutes of the Eighth Flight Control Panel Meeting; Part I - Ascent, February 28, 1974," dated March 12, 1974.

Bending data was prepared and included in the max Q data decks. A Nichols plot of the max Q time point is shown in Figure 26. Bending modes 1 and 9 are unstable by 31.1 and 23.6 db, respectively. Bending modes 2, 3, and 10 are stable but only because they are well phased. Addition of the filters improved modes to 11.5 db unstable, stabilized mode 9 to 16.6 db stable, and destabilized the slosh mode to 3.8 db unstable as shown in Figure 27.

Addition of slosh to bending and bending to slosh coupling produce the effects shown in Figures 28 and 29. The slosh is slightly worse, 3.8 to 4.2 db unstable, as seen in Figures 27 and 29; other changes are slight.

TABLE I. PITCH BENDING DATA AT MAX "Q"

MODE*	1	2	3	6	9	10
Frequency (Rad/Sec) Damping Generalized mass (Kg)	14.09 .005 1,314,034.	16.26 .005 1,314,034.	20.54 .005 1,314,034.	28.71 .005 1,314,034.	39.71 .005 1,314,034.	41.78 .005 1,314,034.
Deflections (M/M) Gimbal 1 Gimbal 2 & 3 Gimbal 4 & 5 Slosh Attach Pt. Acc - Orbitor Acc - SRM	2.806 2.99 -.111 .376 -1.29 -.0573	-.789 -.661 .0134 -.106 -1.97 -.126	-.123 .134 .671 .210 -.283 .837	.0733 .077 -.198 -.0563 .475 -.237	2.025 1.875 .0365 .0122 1.355 .0408	-.0899 -.1127 -.685 .0232 -7.565 -.877
Rotations (Rad/M) Gimbal 1 Gimbal 2 & 3 Gimbal 4 & 5 Slosh Attach Pt. Acc - Orbitor Acc - SRM Rate Gyro-Orbitor Platform	.512 .50 .0277 .50 .00153 .0227 .384 .00153	.190 .190 -.0589 .190 -.133 -.0591 .209 -.133	.0233 .0326 .0698 .0326 -.00334 .0701 .024 -.00334	.0350 .0326 -.0162 .0324 -.0274 -.0163 .018 -.0274	.728 .646 .00174 .646 -.0421 .00176 .146 -.0421	-.1929 -.1768 -.0798 -.1736 .601 -.0803 -.129 .601

*Mode numbers are Rockwell Numbers.

TABLE II. FILTER TRANSFER FUNCTIONS

Attitude Error Filter	$\frac{10.610 S + 1.0}{.183 S^3 + 2.7696S^2 + 29.0323 S + 1.0}$
Attitude Rate Filter	$\frac{.000184 S^3 + .00411 S^2 + .0467 S + 1.0}{.0000132 S^5 + .000353 S^4 + .00506 S^3 + .0486 S^2 + .262 S + 1}$
Acceleration Filter	$\frac{1.0}{2.427 S^2 + 3.2096 S + 1.0}$

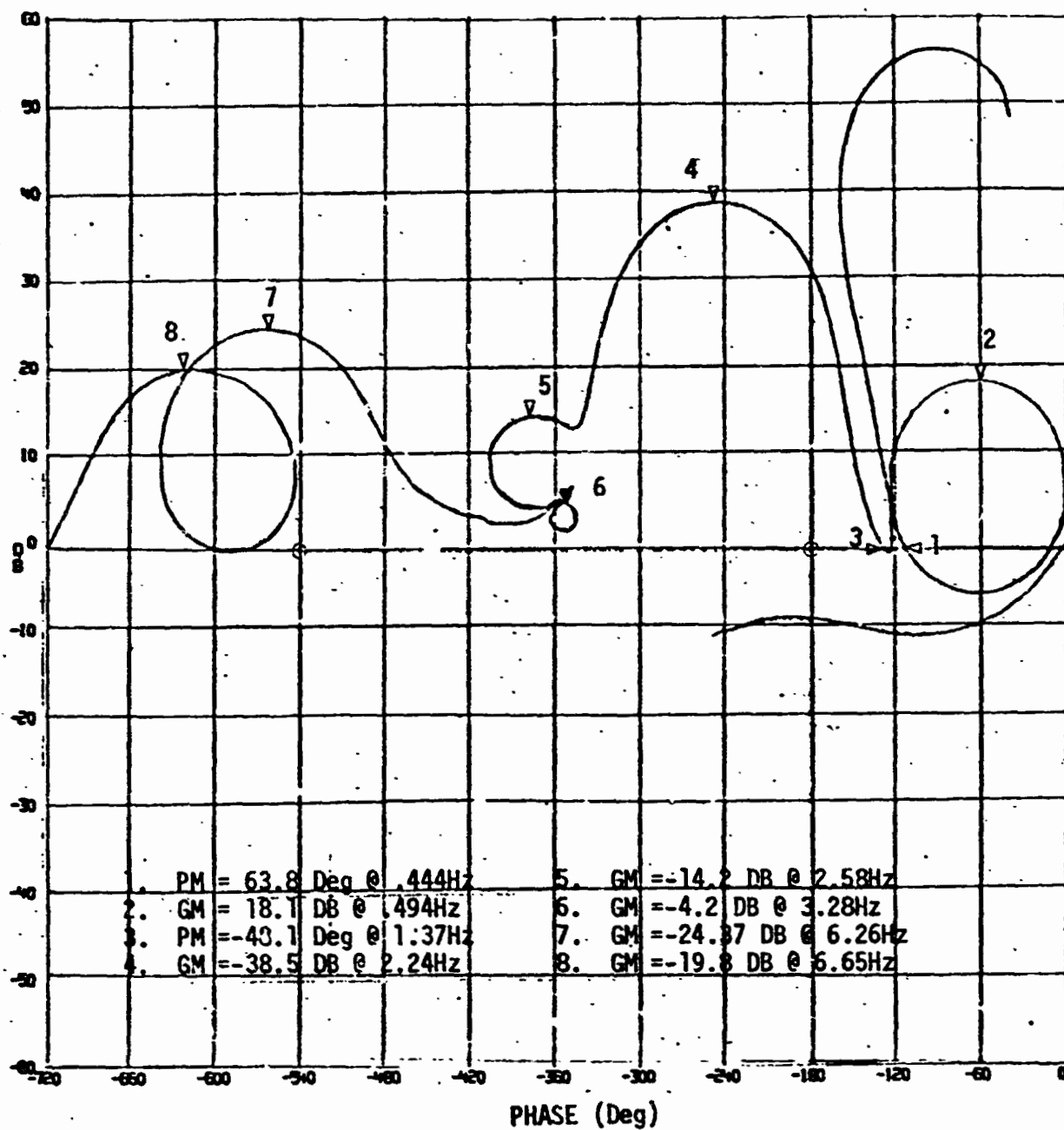


Figure 26 - Pitch Axes Nichols Plot at Max Q-6 Bending Modes

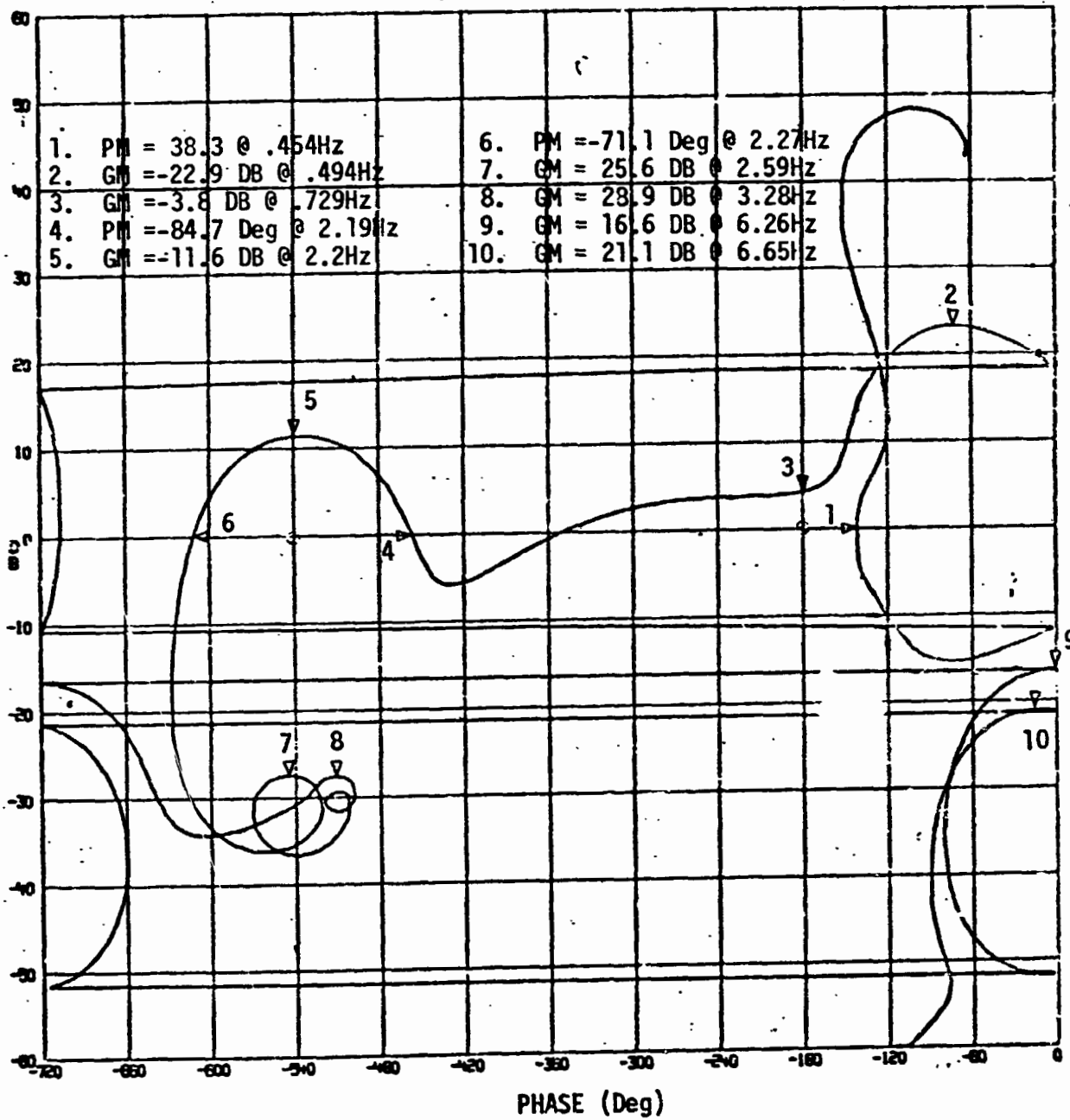


Figure 27 - Pitch Axes Nichols Plot at Max Q-6 Bending Modes - Filters

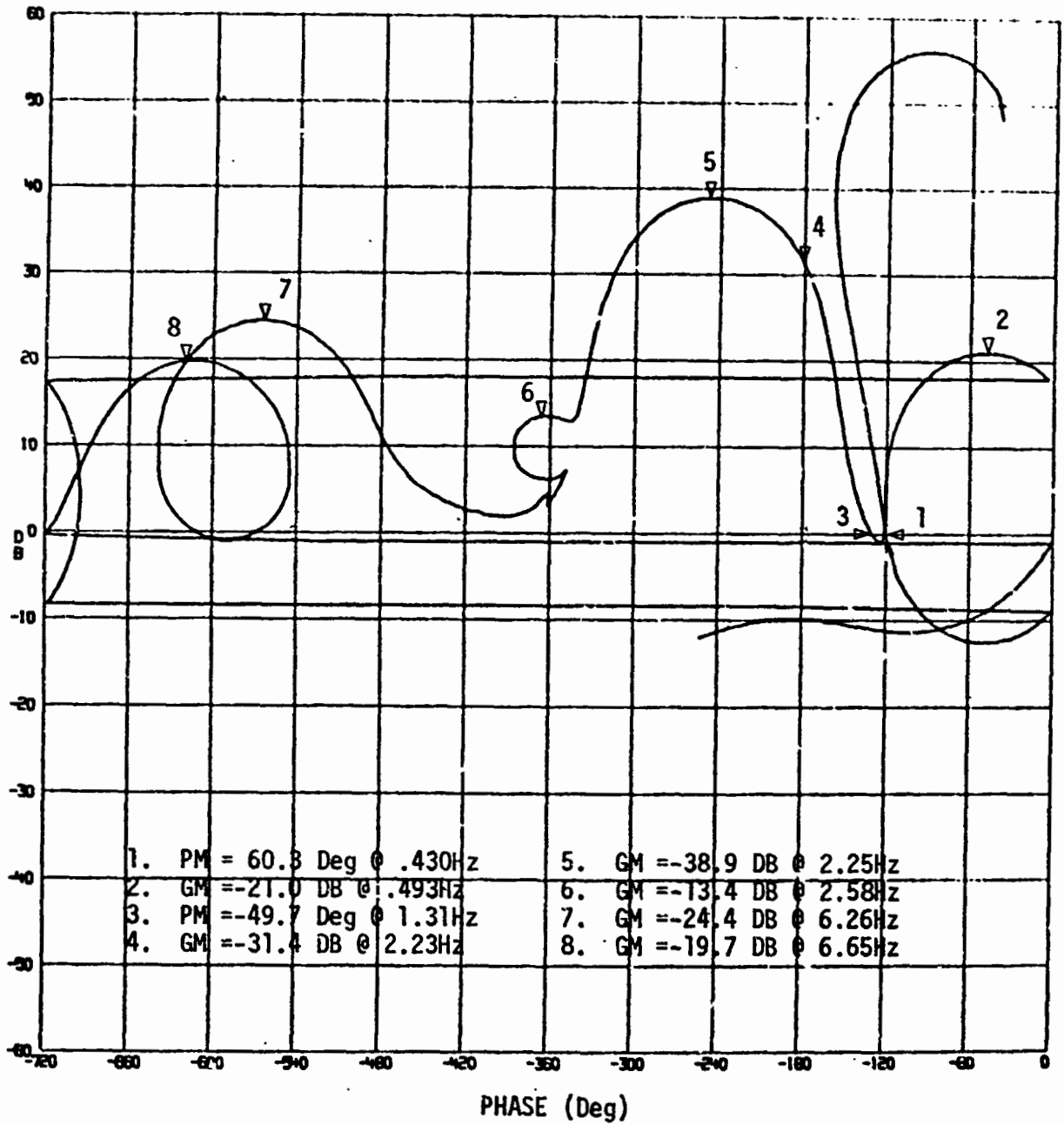


Figure 28 - Pitch Axes Nichols Plot at Max Q-6 Bending Modes - Slosh to Bending and Bending to Slosh

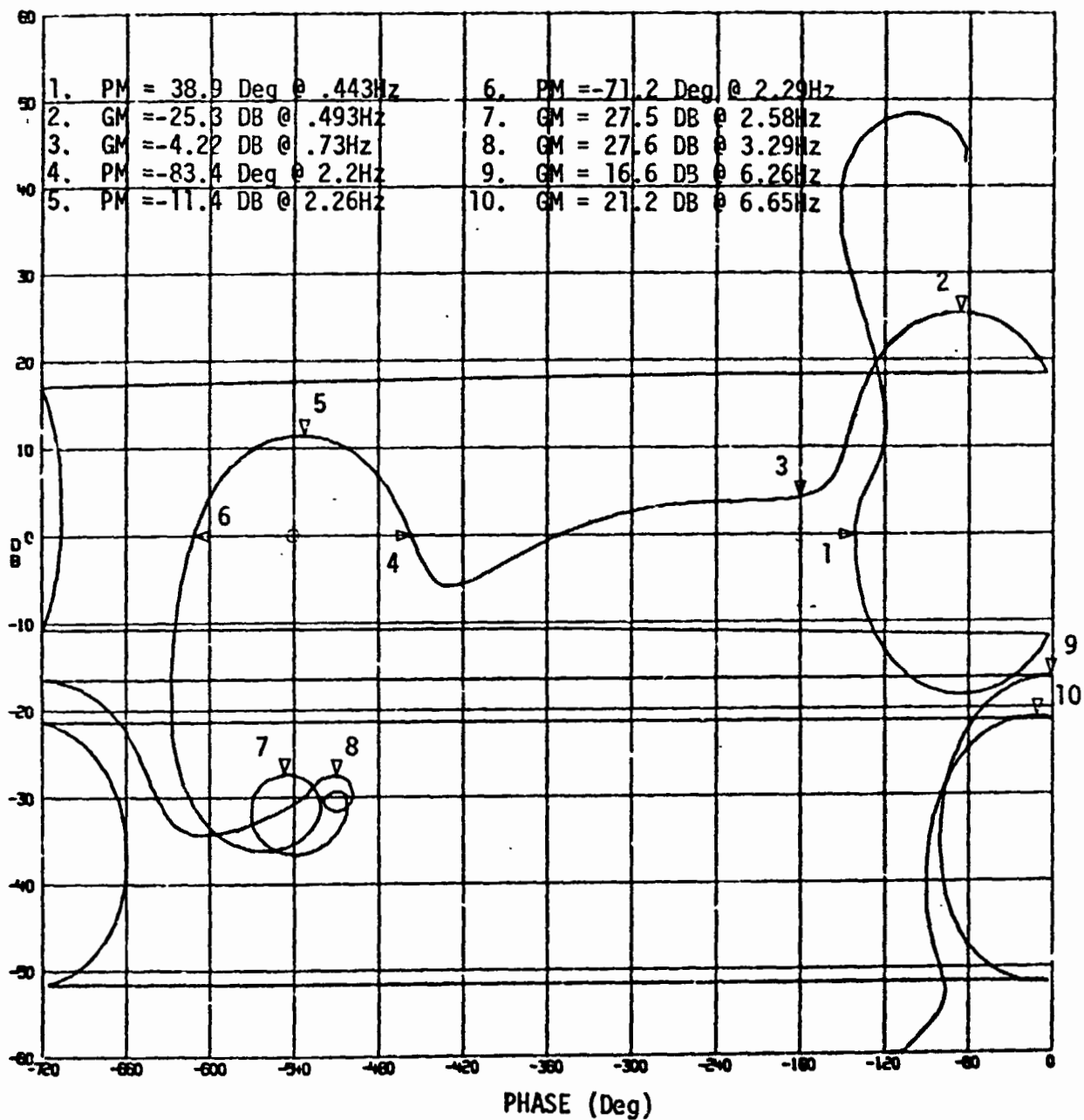


Figure 29 - Pitch Axes Nichols Plot at Max Q-6 Bending Modes - Slosh to Bending and Bending to Slosh - Filters

3.7 DOG WAGS TAIL

3.7.1 Derivation of Actuator Equations

Shuttle actuator equations are presented in the following reference:

MSFC memorandum S&E-ASTP-SD-11-73, "SSME TVC Frequency Response" dated February 15, 1973

Figure 30 shows the block diagram and definition of terms. A transfer function from engine command (β_c) to engine gimbal angle (β_e) is given in the References. The transfer function from external force (F) to engine gimbal angle (β_e) was derived and is given below.

$$\frac{\beta_e}{F} = \frac{A^2 K_1 S (\tau_p S + 1) (\tau_v S + 1) + K_1 K_T K_V K_P \tau_p S + H K_V K_T A (\tau_p S + 1)}{M S^3 A^2 K_1 (\tau_p S + 1) (\tau_v S + 1) + M S^3 K_1 K_T K_V K_P \tau_p + M S^2 H K_V K_T A (\tau_p S + 1) + A^2 K_1 K_T S (\tau_p S + 1) (\tau_v S + 1) + A K_1 K_T K_V H (\tau_p S + 1)}$$

and $\frac{\beta_e}{F}$ in radians/Newton is

$$\frac{\beta_e}{F} = \frac{5.414 \times 10^{-8} [2.229 \times 10^{-4} S^3 + 2.721 \times 10^{-2} S^2 + 1.253 S + 1]}{[8.728 \times 10^{-8} S^5 + 1.065 \times 10^{-5} S^4 + 6.986 \times 10^{-4} S^3 + 2.576 \times 10^{-2} S^2 + 5.50 \times 10^{-1} S + 1]}$$

$$\frac{\beta_e}{F} = W_{fs} \text{ of Section 3.3.}$$

A frequency response plot of W_{fs} is shown in Figure 31.

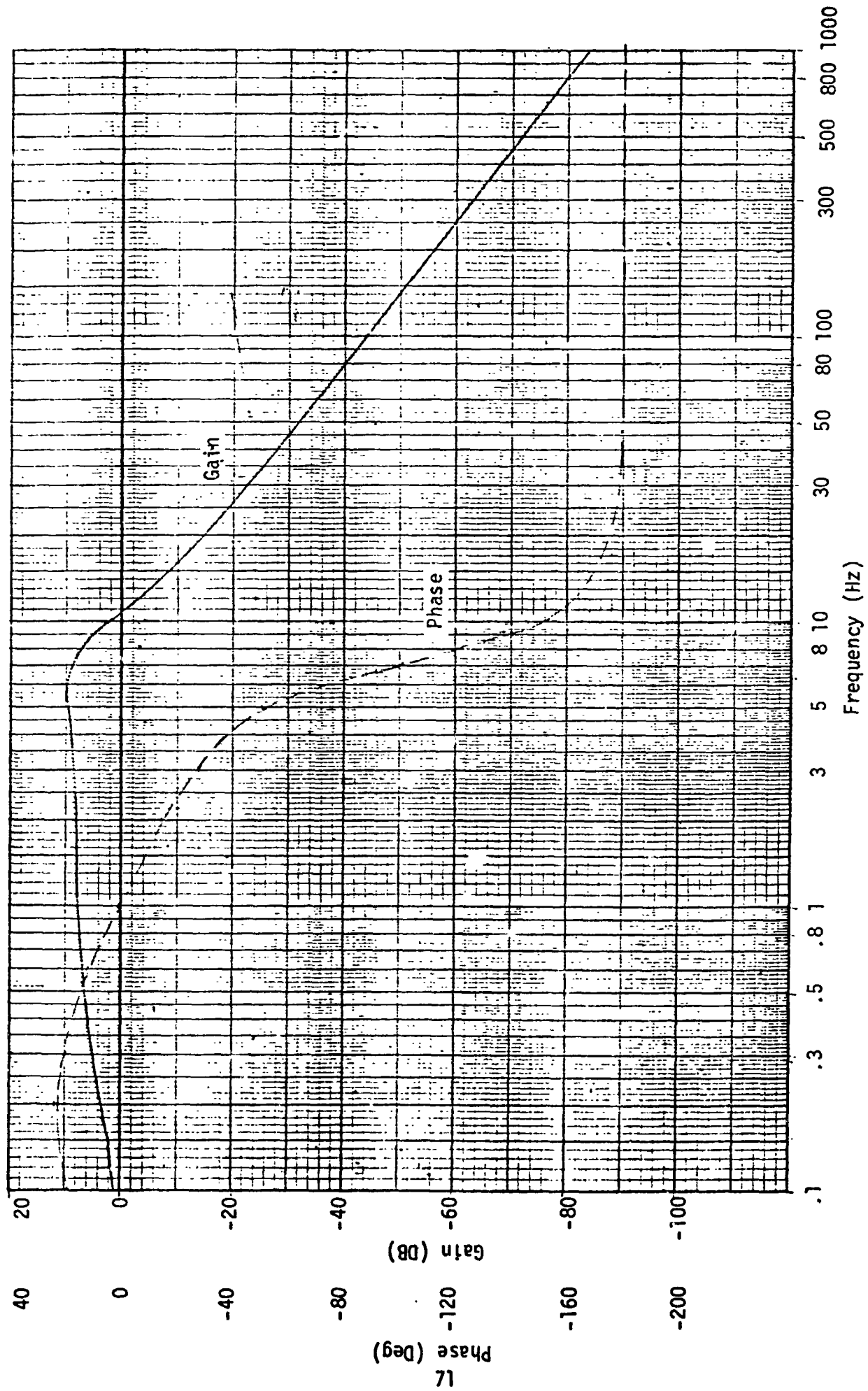


FIGURE 31 FREQUENCY RESPONSE OF DOG WAGS TAIL ACTUATOR TRANSFER FUNCTION

3.7.2 Dog Wags Tail Effect on Vehicle Stability

Dog wag tail terms as discussed in Section 3.7.1 and 3.3.2 were added to the Data Matrices used in Section 3.6. Comparison of Figure 32 with Figure 28 shows the effect produced when Dog Wags Tail terms are added to the uncompensated system. The 9th mode stability is upward from 23.6 to 2.8 DB unstable. First mode stability is upward from 31.4 to 23.0 DB unstable but is phase stable by 47.5 degrees. Closed loop frequencies of the bending modes are increased.

A comparison of Figure 33 with Figure 29 shows the effect produced when Dog Wags Tail terms are added to the compensated system. First mode and higher frequency modes are stabilized while lower frequencies are unaffected.

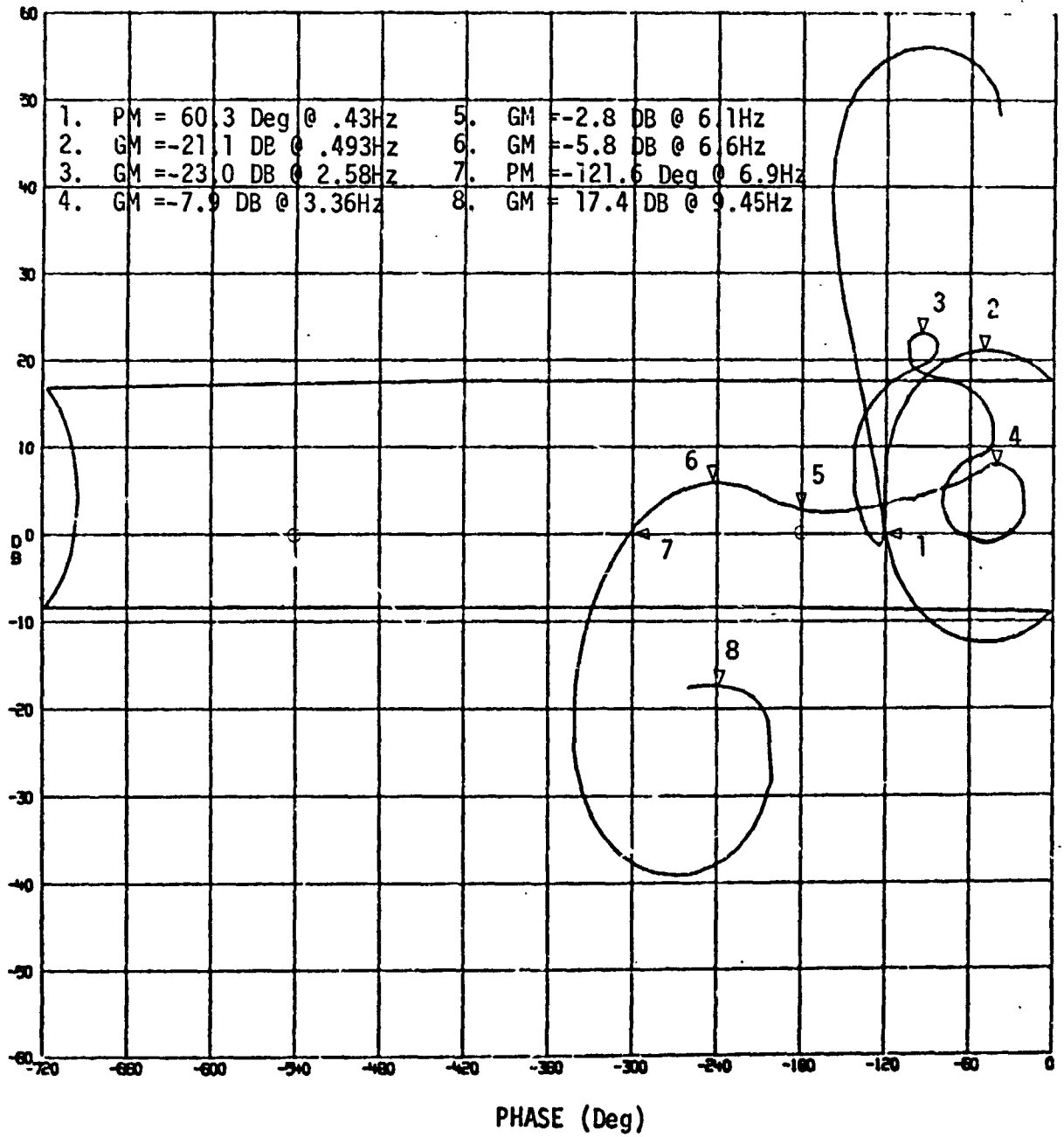


Figure 32 - Pitch Axes Nichols Plot at Max Q-6 Bending Modes - Slosh to Bending and Bending to Slosh - DWT

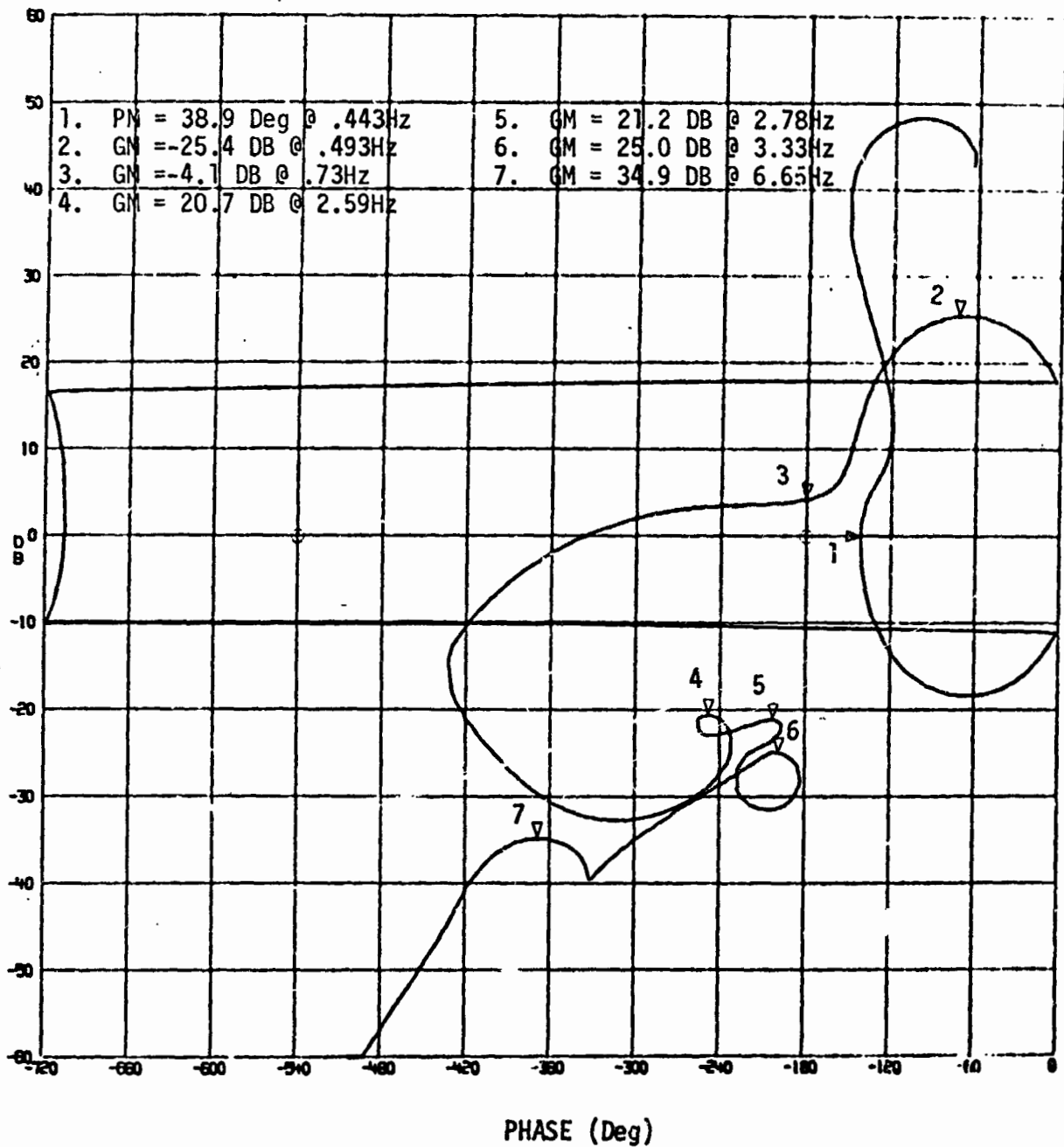


Figure 33 - Pitch Axes Nichols Plot at Max Q-6 Bending Modes - Slosh to Bending and Bending to Slosh - DWT - Filters

4.0 GUIDANCE ANALYSIS

The original powered flight guidance software proposed for Shuttle consisted of several specialized routines to handle the various phases of flight (as Saturn V/Apollo). The Boeing developed Linear Tangent Guidance (LTG) equations were baselined for Shuttle nominal ascent. Investigation revealed that Apollo-type guidance was inadequate to handle some phases of Shuttle flight (i.e., low thrust deorbit). It was later discovered by the Mission Planning and Analysis Division (MPAD) of JSC that the basic LTG algorithm was accurate and flexible enough to handle some of these difficult phases. MPAD then developed the concept of extending the basic ascent LTG equations to handle all phases of Shuttle powered flight, including Abort Once Around (AOA) and Return to Launch Site (RTLS) abort. Brand, Brown, and Higgins of the Massachusetts Institute of Technology (MIT) later developed concepts that made it feasible to extend the ascent LTG to handle various phases of Shuttle flight.

The basic Boeing guidance task under this contract was to coordinate with MPAD, MIT and Rockwell International Corporation in development of the Unified Linear Tangent Guidance (ULTG) and to implement this capability in the JSC Space Shuttle Functional Simulator (SSFS). Emphasis was placed on abort capability. Various candidate abort techniques were critiqued. It was determined that all of the existing candidates for RTLS abort guidance had certain limitations and disadvantages. As a result, Boeing developed a complete solution to the RTLS abort problem satisfying all constraints and compatible with the ULTG as a simple option (Section 5.0, Volume V). In order to solve the RTLS problem, the original LTG algorithm was significantly modified. A unified optimum guidance algorithm, involving higher order accuracy and more flexibility, was developed. This accuracy and flexibility made range throttling possible and made it possible for the steering to modulate to deplete excess propellant and simultaneously satisfy velocity and position constraints (during RTLS powered flight).

The guidance work performed under this contract, and documented in Volume V, contributes to all phases of Shuttle powered flight guidance. A technique for handling the Orbiter Maneuvering System (OMS) ascent phase was developed

and is presented in Section 4.1. This technique has been implemented in the ULTG of the SSFS and incorporated into the currently baselined Shuttle powered flight guidance equations. Theoretical background and development of the unified optimum guidance algorithm are presented in Sections 2.0 and 3.0 of Volume V. Methods of handling various sets of end-conditions are presented in Section 4.0. Two explicit powered flight guidance algorithms for RTLS are presented in Section 5.0. And finally, Section 6.0 contains a method for implementing the steering computations for all Shuttle phases. RTLS time-to-go and range throttling equations are also included. The RTLS powered flight option is presently being programmed in the SSFS by NASA-JSC and LEC.